Available online at www.sciencedirect.com
SCIENCE DIRECT®
International Journal of Multiphase Flow 30 (2004) 239–272
International Journal of Multiphase Flow
www.elsevier.com/locate/ijmulflow

Modelling of gas entrainment from Taylor bubbles. Part A: Slug flow

N. Brauner *, A. Ullmann

Department of Fluid Mechanics and Heat Transfer, Faculty of Engineering, Tel Aviv University, Tel Aviv 69978, Israel

Received 1 September 2002; received in revised form 24 November 2003

Abstract

A model that attributes the aeration of the liquid slug to a recurrent bubble entrainment from the Taylor bubble (TB) tail is introduced. The bubble fragmentation is related to the rate of turbulent kinetic energy produced in the wall jet and shear layer, which are formed in the TB wake as the liquid film plunges into the slug front. The bubble fragmentation model has been incorporated into a complete model, which suggests a unified method for the prediction of the slug void fraction and other slug characteristics in horizontal, inclined and vertical slug flow. The model has been tested against experimental data available from the literature and was found to predict the effects of liquid and gas flow rates and their physical properties, as well as tube diameter and inclination.

Keywords: Slug flow; Holdup; Entrainment; Taylor bubble; Gas–liquid; Aeration

1. Introduction

Correlations or models for the prediction of the in situ void fraction of liquid slugs in horizontal, inclined and vertical tubes are required as a closure relationship for the modelling of gas–liquid slug flow. The evaluation of the liquid slug holdup is important in particular for the design of vertical and off-vertical inclined systems, since the hydrostatic pressure drop is practically determined by the liquid holdup in the slug.

Several attempts to suggest an experimental correlation for evaluating the void fraction in the slug were reported in the literature. A widely used correlation is that of Gregory et al. (1978),

* Corresponding author. Tel.: +972-3-640-8127/8930; fax: +972-3-640-7334.
E-mail address: brauner@eng.tau.ac.il (N. Brauner).

0301-9322/$ - see front matter
doi:10.1016/j.ijmultiphaseflow.2003.11.007

which suggests a dependence only on the mixture velocity. Other studies, however, indicate a dependence of the slug void fraction on the liquid-cut in the feed (Dukler and Hubbard, 1975; Greskovich and Shrier, 1971; Heywood and Richardson, 1979), on the fluid properties (Malnes, 1982; Ferschneider, 1983) and on the pipe inclination (Andreussi and Bendiksen, 1989; Felizola and Shoham, 1995; Nuland et al., 1997; Gomez et al., 2000). Only a few studies attempt to model the entrainment of gas bubbles from the Taylor bubble (TB) tail into the liquid slug. The models of Fernandes et al. (1983) for vertical slug flow and those of Andreussi and Bendiksen (1989) and Nydal and Andreussi (1991) for nearly horizontal slug flow, relate the gas entrainment to the relative velocity between the gas in the Taylor bubble and liquid film. However, the model of Fernandes et al. (1983) ignores the effect of surface tension, which must play a role in bubble fragmentation, while in the other models surface tension effect was introduced only through an empirical relation for the critical mixture velocity for the onset of bubbles entrainment.

A different approach to model the void fraction in the slug was suggested by Barnea and Brauner (1985). Their model attributes the slug aeration to the turbulence in the slug bulk. It assumes that the gas in developed liquid slugs appears as fully dispersed bubbles, and that the in situ gas fraction is the same as the gas fraction on the slug/dispersed-bubble transitional boundary for the same total mixture velocity, U_m. The possibility of predicting the variation of the gas fraction in liquid slugs with the system's parameters via this model is thus dependent on the availability of robust models for predicting the conditions for transition from slug flow to dispersed-bubble flow in various gas–liquid systems. The model has been found to be in a good agreement with experimental data taken in relatively long liquid slugs, particularly in horizontal tubes. However, in vertical slug flow and high mixture velocities, this model has been found to underestimate the measured gas fraction in the liquid slug (Barnea and Shemer, 1989).

The approach of Barnea and Brauner (1985) was retested in Brauner and Ullmann (2002) by employing the models for the prediction of transition to dispersed flows (Brauner, 2001). These models are based on an extension of the Kolmogorov (1949)–Hinze (1955) theory for break-up of droplets/bubbles in a turbulent field to the case of dense dispersions. When these models are combined with the Barnea and Brauner (1985) procedure, analytical expressions are obtained for the slug void fraction. These are summarized in Table 1. It was shown that the expressions obtained are of the same form as the experimental correlation of Gregory et al. (1978), which was obtained for a particular gas–oil system. The controlling dimensionless parameters are the slug Weber number ($\rho_L D U_m^2/\sigma$), Reynolds number ($\rho_L D U_m/\eta_L$) and the Eötvös number

Table 1
Slug void fraction based on turbulence in the slug bulk (SLB model)

Eo_D	ε_{LS}	$(U_m)_{crit}$
>5	$\frac{0.022C_H^{-1}\,We_s f_s^{2/3}(Eo_D\cos\beta')^{-5/6}}{1+0.022C_H^{-1}\,We_s f_s^{2/3}(Eo_D\cos\beta')^{-5/6}}$	$2.65\left\{\frac{(\lvert\Delta\rho\rvert g\cos\beta')^{0.5}\sigma^{0.1}}{\rho_L^{0.52}\eta_L^{0.08}}D^{0.48}\right\}^{0.893}$
<5, >0.2	$\frac{0.028C_K^{-1}\,We_s f_s(Eo_D\cos\beta')^{-0.5}}{1+0.028C_K^{-1}\,We_s f_s(Eo_D\cos\beta')^{-0.5}}$	$8.53\left[\frac{(\sigma\Delta\rho g\cos\beta')^{0.5}D^{0.2}}{\rho_L^{0.8}\eta_L^{0.2}}\right]^{0.55}$
<0.2	$\frac{0.25C_K^{-1}\,We_s f_s}{1+0.25C_K^{-1}\,We_s f_s}$	$9.72\left(\frac{\sigma}{\rho_L^{0.8}\eta_L^{0.2}D^{0.8}}\right)^{0.55}$

$We_s=\frac{\rho_L U_m^2 D}{\sigma}$; $f_s=\frac{0.046}{Re_s^{0.2}}$; $Re_s=\frac{\rho_L U_m D}{\eta_L}$; $(We_s)_{crit}=\frac{\rho_L D(U_m^2)_{crit}}{\sigma}$; C_H, $C_K=O(1)$ tuned const; β'-Eq. (6.2).

$Eo_D = \Delta\rho g D^2/8\sigma$. However, the variation with the tube inclination indicated by these model expressions is mild, since gravity has a minor role in determining the conditions for transition to fully dispersed flow pattern. It can be argued that such models are applicable to the prediction of the gas fraction in long liquid slugs and short TB. Indeed, in horizontal slug flow, where the liquid-cut (U_{ws}/U_m) in the feed is relatively high, the dispersive forces are expected to be of the same order of magnitude as in the continuous liquid phase on the verge of dispersed-bubbles/slug flow transition.

In general, the aeration of the liquid slug is affected by the dispersion mechanisms taking place at the TB tail and its wake in front of the slug. In the front of the liquid slug, the dispersive forces are due to the wall jet and shear layer formed at the Taylor bubble wake (TBW), as a result of the relative velocity between the liquid in the slug front and the plunging liquid film at the TB tail. A significant effect of the tube inclination on the rate of bubble entrainment results from the sensitivity of the liquid film velocity to the inclination.

The TBW model is presented in the next section and the calculation procedure in Section 3. The model predictions for vertical, inclined and horizontal slug flow are discussed in Section 4 and tested against experimental data available form the literature. The TBW model is shown to predict the effects of the fluids flow rates, the physical properties, tube diameter and inclination, as well as the effect of the TB length on the rate of bubble entrainment. In a subsequent paper (Brauner and Ullmann, 2004), the model is modified for the case of bubble entrainment from a stationary TB.

2. The Taylor bubble wake (TBW) model

The idealized physical pictures of slug flow in vertical and inclined (or horizontal) tubes are described in Fig. 1a and b respectively. In these figures, section 'w' represents the near TB wake region and section 's' the far wake region in the liquid slug. The gas in the Taylor (elongated) bubble (TB) moves at a velocity U_{GTB}, which is faster than the average velocity in the liquid slug, the mixture velocity, U_m. Therefore, material is shed from the back of the slug to form the falling film (or a liquid trail) along the TB. The liquid in the film at the TB nose may be aerated, with ε_{GLf} representing its void fraction. However, the small bubbles, which are dispersed in the preceding slug, coalesce with the TB interface and are gradually absorbed into the TB. Eventually, the liquid film becomes practically un-aerated. Simultaneously, bubbles are re-entrained from the TB tail into the TB wake at a rate Φ_{Ge}. Part of the bubbles that are entrained into the TB wake may re-coalesce with the TB tail (at a rate Φ_{Gb}), resulting in a net gas flow rate of $\Phi_{Ge} - \Phi_{Gb}$ out of the TB tail. This net rate is shed upstream to the successive TB.

The flow phenomena in the TB near and far wake regions are different. Typically, the in situ gas fraction in the TB wake region, ε_{LS}^{w} is higher than the in situ gas fraction within the liquid slug, ε_{LS}^{s}. In a stable slug flow, the slug length, L_{LS} and the TB length, L_{TB} remain essentially constant in the downstream direction. Hence, $\Phi_{GS} = \Phi_{Ge} - \Phi_{Gb}$ is the constant gas flow rate which is shed backward in coordinate system attached to the TB, and eventually is absorbed into the successive TB. The recurrent bubble entrainment from the TB tail and their re-coalescence at the successive TB nose result in an effective TB translation velocity, $U_{T\varepsilon}$, which is higher than the gas velocity in the TB, U_{GTB}.

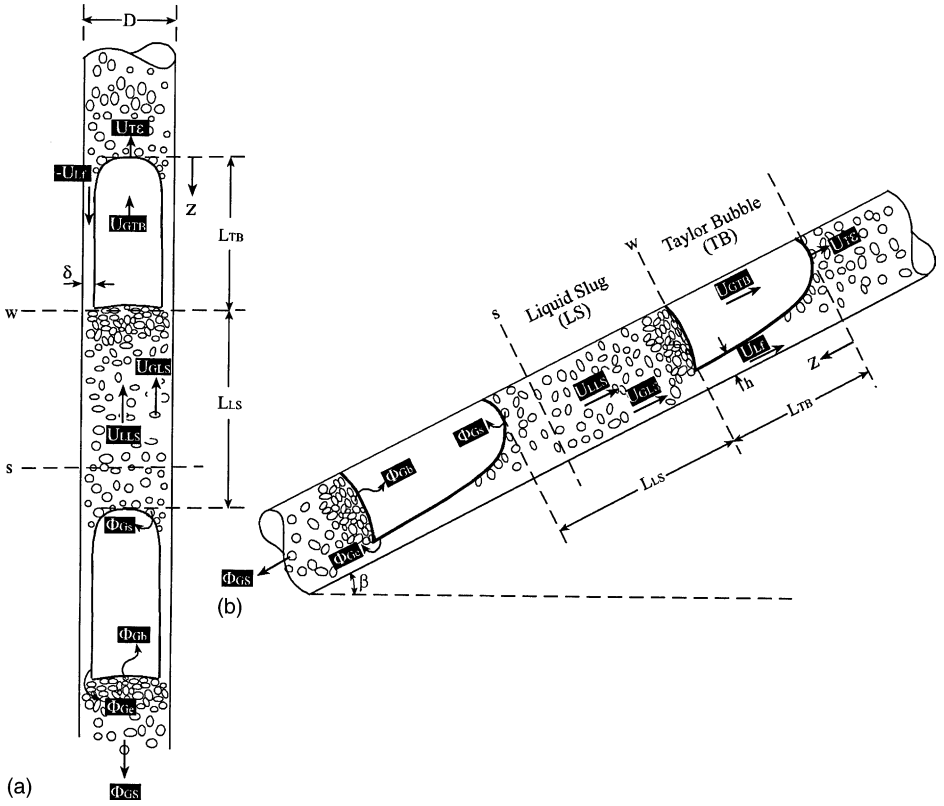

Fig. 1. Schematic description of the TBW model for slug flow: (a) vertical tube; (b) inclined tube.

The fragmentation of the TB tail and the entrainment of the bubbles into the TB wake are due to the dispersing forces induced by the flow of the liquid film as it plunges into the liquid slug front. This combined process of fragmentation of the TB tail and bubble entrainment into the slug is in fact a non-stationary process. It involves a disordered and intermittent expansion of the tail followed by its fragmentation. A relevant turbulent model for characterizing the dispersive forces is that associated with a wall jet and shear layer formed in the liquid slug front, due to the relative velocity between the liquid in the slug front (moving at velocity $U_{\mathrm{LLS}}^{\mathrm{w}}$) and the liquid film at the tail of the preceding TB (moving at velocity $U_{\mathrm{Lf}}^{\mathrm{w}}$). Therefore, the modelling of the in situ gas fraction in the slug is coupled with the modelling of all other hydrodynamic variables characterizing the slug flow.

2.1. Bubble entrainment from the Taylor bubble (TB) tail

The flux of surface energy production due to fragmentation of the TB tail into bubbles at a rate Φ_{Ge} is given by:

$$\dot{E}_{\mathrm{s}} = \frac{\pi d_{32}^2 \sigma}{\pi d_{32}^3/6}\,\Phi_{\mathrm{Ge}} = \frac{6\sigma}{d_{32}}\,\Phi_{\mathrm{Ge}} \tag{1}$$

where σ is the surface tension and d_{32} is the Sauter mean bubble diameter. The d_{32} can be scaled with reference to the maximal bubble size, $d_{32} = d_{\max}/k_d$. The flux of this surface energy production is proportional to the flux of turbulent energy supply by the penetrating liquid film "jet" at a rate Φ_{Lf}:

$$\frac{1}{2}\rho_{\mathrm{L}}(u'^2 + v'^2 + w'^2)\Phi_{\mathrm{Lf}} = C_{\mathrm{J}}\frac{6\sigma}{d_{\max}}\Phi_{\mathrm{Ge}} \tag{2}$$

where

$$\Phi_{\mathrm{Lf}} = (U_{\mathrm{GTB}} - U^{\mathrm{w}}_{\mathrm{Lf}})(1 - \varepsilon^{\mathrm{w}}_{\mathrm{TB}}) \tag{3}$$

C_{J} is a constant, $C_{\mathrm{J}} = \mathrm{O}(1)$ (which embodies the scaling constant, k_d) and U_{GTB} is the gas velocity in the TB, which is also the velocity of an unfragmented TB tail. Note that the latter is used in Eq. (3) (rather than $U_{\mathrm{T}\varepsilon}$) to represent the film flux responsible for the fragmentation of the TB tail. This is in order to account for the periodic and sequential nature of the local phenomena involving film penetration and TB expansion, which are then followed by the tail fragmentation.

The turbulent field is that associated with a wall jet and a shear layer formed in the slug front (TB wake) between the liquid bulk moving at a velocity $U^{\mathrm{w}}_{\mathrm{LLS}}$ and the liquid film moving at velocity $U^{\mathrm{w}}_{\mathrm{Lf}}$ (see Fig. 1). The maximal values reported for compound shear layers are $u'^2 \simeq 0.03\,\Delta U^2$, $v'^2 \simeq 0.02\,\Delta U^2$, $w'^2 \simeq 0.013\,\Delta U^2$ (Rajaratnam, 1976). Recent data of the velocity field in the wake of a single TB rising through stagnant water in a vertical pipe (Van Hout et al., 2002a,b) indicates even higher u' and v' close to the TB tail. Here, conservative values of $u'^2 \simeq v'^2 \simeq w'^2 \cong 0.01\,\Delta U^2$ are taken, thus

$$u'^2 + u'^2 + w'^2 \simeq 0.03(U^{\mathrm{w}}_{\mathrm{LLS}} - U^{\mathrm{w}}_{\mathrm{Lf}})^2 \tag{4}$$

Recent experiments on gas entrainment from the tail of a stationary bubble (e.g. Hernandez-Gomez and Fabre, 2001; Delfos et al., 2001) substantiate the observations made in slug flow, that gas entrainment occurs provided the bubble length, hence the film velocity, exceeds a certain threshold value. The threshold value on the film velocity can be estimated assuming it corresponds to a critical Weber number of the order of unity:

$$We'_{\mathrm{crit}} = \frac{\rho_{\mathrm{L}} d_{\max}(u'^2 + v'^2 + w'^2)_{\mathrm{crit}}}{3\sigma} = C' \simeq \mathrm{O}(1) \tag{5}$$

The maximal stable bubble size in a swarm (Barnea, 1987; Brauner, 2001) is estimated based on the critical size of deformable bubbles suggested by Brodkey (1969):

$$\tilde{d}_{\max} \simeq \tilde{d}_{\mathrm{crit}} = \frac{d_{\mathrm{crit}}}{D} = \left[\frac{0.4\sigma}{(\rho_{\mathrm{L}} - \rho_{\mathrm{G}})g\cos\beta' D^2}\right]^{1/2} = \frac{0.224}{(\cos\beta' Eo_D)^{1/2}} \tag{6.1}$$

$$Eo_D = \frac{\Delta\rho g D^2}{8\sigma}; \quad \beta' = \begin{cases} |\beta|; & |\beta| \leqslant 45^\circ \\ 90 - |\beta|; & |\beta| > 45^\circ \end{cases} \tag{6.2}$$

Note that in capillary systems, $Eo_D \ll 1$, where Eq. (6.1) yields $\tilde{d}_{\mathrm{crit}} > 1$, the maximal drop size is scaled with reference to the tube diameter to represent a minimal distance required for maintaining separated bubbles in a dispersed pattern ($\tilde{d}_{\max} < \tilde{d}_{\mathrm{crit}} \simeq 0.25$ is used).

Assuming that only the excess of the turbulent kinetic energy above that corresponding to We'_{crit} is responsible for the bubble fragmentation, and using Eqs. (4)–(6) in Eq. (2) results in

$$\frac{\Phi_{\mathrm{Ge}}}{\Phi_{\mathrm{Lf}}} = \frac{1}{400 C_{\mathrm{J}}} \tilde{d}_{\mathrm{crit}} (We - We_{\mathrm{c}}); \quad We \geqslant We_{\mathrm{c}} \tag{7.1}$$

$$We = \frac{\rho_{\mathrm{L}} D (U^{\mathrm{w}}_{\mathrm{LLS}} - U^{\mathrm{w}}_{\mathrm{Lf}})^2}{\sigma}; \quad We_{\mathrm{c}} = \frac{100 C'}{\tilde{d}_{\mathrm{crit}}} \tag{7.2}$$

For instance, in atmospheric air–water flow in 5.1 cm pipe, $\tilde{d}_{\mathrm{crit}} \simeq 0.033$, whereby $We_{\mathrm{c}} \simeq 2000$. In fact, C_{J} and C' are tunable constants. The tuning of C_{J} can also account for the combined effects of inaccuracies introduced by the estimated numeric constants used in the various sub-models (e.g. turbulence intensity, critical bubble size). In this study, the model is applied with $C_{\mathrm{J}} = 1$, $C' = 2/3$. This value is found to be in agreement with the data of Nydal and Andreussi (1991) on aeration of a liquid body advancing over a slow moving liquid layer in a nearly horizontal 5 cm pipe (when their critical velocity difference is presented in terms We_{c}). However, for bubble fragmentation in homogeneous turbulent field, the critical Weber number was found to decrease with increasing $\rho_{\mathrm{G}}/\rho_{\mathrm{L}}$ (Sevik and Park, 1973; Zaichik et al., 2002). Therefore, lower C' should be considered when the model is applied to high pressure/dense gas systems.

It is worth mentioning at this point that while $U^{\mathrm{w}}_{\mathrm{LLS}} > 0$, the sign of $U^{\mathrm{w}}_{\mathrm{Lf}}$ depends on the tube inclination and the distance from the TB nose. For a steep upward inclination, $U^{\mathrm{w}}_{\mathrm{Lf}}$ is practically always negative (downward, except at the TB nose region).

2.2. Liquid and gas velocities in the slug

The bubbly flow in the slug region can be described by the drift-flux model. The bubbles and liquid velocities in the TB wake, $U^{\mathrm{w}}_{\mathrm{GLS}}$, and $U^{\mathrm{w}}_{\mathrm{LLS}}$ are given by

$$U^{\mathrm{w}}_{\mathrm{GLS}} = C^{\mathrm{w}}_0 U_{\mathrm{m}} + U^{\mathrm{w}}_0 \tag{8.1}$$

and

$$U^{\mathrm{w}}_{\mathrm{LLS}} = \frac{U_{\mathrm{m}} - \varepsilon^{\mathrm{w}}_{\mathrm{LS}} U^{\mathrm{w}}_{\mathrm{GLS}}}{(1 - \varepsilon^{\mathrm{w}}_{\mathrm{LS}})} \tag{8.2}$$

The distribution parameter, defined as $C^{\mathrm{w}}_0 = \frac{(\overline{u_{\mathrm{m}}\varepsilon})^{\mathrm{w}}}{U_{\mathrm{m}}\varepsilon^{\mathrm{w}}_{\mathrm{LS}}}$ (ε and u_{m} are the local gas fraction and mixture flux), accounts for the bubble concentration and velocity profiles (see the discussion in Section 3). For the drift velocity, U^{w}_0, the Harmathy's (1960) model corrected for the effect of the swarm (Wallis, 1969) and tube inclination is used:

$$U^{\mathrm{w}}_0 = 1.53 \left[\frac{\sigma g (\rho_{\mathrm{L}} - \rho_{\mathrm{G}})}{\rho^2_{\mathrm{L}}} \right]^{0.25} \sin\beta (1 - \varepsilon^{\mathrm{w}}_{\mathrm{LS}})^{1.5} \tag{8.3}$$

Upstream, in the TB far wake region, where the wake effects diminish, the liquid and gas velocities $U^{\mathrm{s}}_{\mathrm{LLS}}$ and $U^{\mathrm{s}}_{\mathrm{GLS}}$ are obtained using Eqs. (8) with superscript 's' replacing superscript 'w' everywhere:

$$U^{\mathrm{s}}_{\mathrm{GLS}} = C^{\mathrm{s}}_0 U_{\mathrm{m}} + U^{\mathrm{s}}_0 \tag{9.1}$$

and

$$U^{s}_{LLS} = \frac{U_m - \varepsilon^{s}_{LS} U^{s}_{GLS}}{(1 - \varepsilon^{s}_{LS})} \tag{9.2}$$

2.3. The TB translation velocity and the gas fraction in the slug

The average gas velocity in the TB is considered to be practically unaffected by the small bubbles absorbed at the TB interface and their re-entrainment at the TB tail. Hence, it is determined by the TB rise velocity, which is expressed by Nicklin et al. (1962) equation:

$$U_T = C_0^{TB} U_m + U_0^{TB} = U_{GTB} \tag{10}$$

where C_0^{TB} is the velocity distribution parameter ($\simeq$1.2 for turbulent flow in an un-aerated slug, see the discussion in Section 3) and U_0^{TB} is the rise velocity of the TB in stagnant liquid. The latter is dependent on the tube inclination and capillary number $\Sigma = \frac{4\sigma}{\Delta\rho g D^2}$ (or the Eötvös number, e.g. Zukoski, 1966; Fabre and Liné, 1992). In gravity dominated systems and in the inertia controlled regime:

$$\frac{U_0^{TB}}{\left(\frac{\Delta\rho}{\rho_L} gD\right)^{1/2}} = C_v^{TB} = 0.35; \quad \beta = 90^\circ, \ \ \Sigma \to 0 \tag{11.1}$$

$$\frac{U_0^{TB}}{\left(\frac{\Delta\rho}{\rho_L} gD\right)^{1/2}} = C_h^{TB} = 0.54; \quad \beta = 0^\circ, \ \ \Sigma \to 0 \tag{11.2}$$

In inclined systems, the weighted value suggested by Bendiksen (1984) is used:

$$\frac{U_0^{TB}}{\left(\frac{\Delta\rho}{\rho_L} gD\right)^{1/2}} = C_v^{TB} \sin\beta + C_h^{TB} \cos\beta \tag{12}$$

It is to be noted that in a vertical tube, C_v^{TB} reaches the limiting value of 0.35 for $\Sigma \simeq 0.1$ ($Eo_D \simeq 5$). Based on the data of Zukoski (1966), correlations for the decline of C_v^{TB} with Σ in systems of low Eo_D in the inertia controlled regime ($Re_{TB} \gg 10$) and in the viscous controlled regime, are given in Appendix A. For horizontal tubes and in the inertia controlled regime, the correlation obtained by Weber (1989) for the data of Zukoski (1966) is applied ($C_h^{TB} = 0.54 - 0.55 Eo_D^{-0.56}$).

Part of the bubbles that are entrained from the TB may re-coalesce with its tail. Since the instantaneous velocity field as visualized in the TB wake region is very disordered, the average bubble back-flow may be also a result of the instantaneous velocity components. Here, however, the bubbles back-flow is estimated based on the difference between the drift velocity of the TB and that of the bubbles in the swarm:

$$\Phi_{Gb} = \begin{cases} (U_0^{w} - U_0^{TB}) \varepsilon^{w}_{LS} \varepsilon^{w}_{TB}; & U_0^{w} > U_0^{TB} \\ 0; & U_0^{w} \leqslant U_0^{TB} \end{cases} \tag{13}$$

Since in most practical applications the TB drift is higher than that of the bubbles in the swarm, the above back-flow model has a minor or no effect on the predicted slug flow structure. A more

rigorous model for the back-flow requires details of the flow phenomena in the TB wake. In case of $\Phi_{Gb} > 0$, the net averaged rate of gas loss from the TB tail, which is shed out of the TB wake region into the liquid slug (and the successive TB nose) is:

$$\Phi_{GS} = \begin{cases} \Phi_{Ge} - \Phi_{Gb}; & \Phi_{Ge} > \Phi_{Gb} \\ 0; & \Phi_{Ge} \leqslant \Phi_{Gb} \end{cases} \tag{14}$$

Following the above assumptions, both ε^{w}_{LS} and ε^{s}_{LS} are calculated from a mass balance on the gas in a coordinate system attached to the TB transitional velocity, $U_{T\varepsilon}$. For a non-negligible slip between the liquid and the gas in the slug, U_{GLS} is dependent on the in situ gas fraction (see Eqs. (8) and (9)). Therefore, the corresponding equations are written in the implicit form:

$$\varepsilon^{w}_{LS} - \frac{\Phi_{GS}}{U_{T\varepsilon} - U^{w}_{GLS}} = 0 \tag{15.1}$$

$$\varepsilon^{s}_{LS} - \frac{\Phi_{GS}}{U_{T\varepsilon} - U^{s}_{GLS}} = 0 \tag{15.2}$$

Also, in developed slug flow and in case the film at the TB tail is un-aerated:

$$\Phi_{GS} = \varepsilon^{w}_{TB}(U_{T\varepsilon} - U_{GTB}) \tag{16}$$

Since $U_{GTB} = U_T$ (see Eq. (10)), Eq. (16) indicates that in case of recurrent coalescence of bubbles from the liquid slug with the TB nose and their re-entrainment from the TB tail at a rate $\Phi_{GS} > 0$, the TB translation velocity exceeds the TB rise velocity in un-aerated slug flow (see also Dukler et al., 1985), whereby

$$U_{T\varepsilon} = U_T + \frac{\Phi_{GS}}{\varepsilon^{w}_{TB}} \tag{17.1}$$

Alternatively, combining Eq. (16) with Eqs. (9.1) and (15.2) yields:

$$\Delta U_T = U_{T\varepsilon} - U_T = \frac{[U_m(C^{TB}_0 - C^{s}_0) + U^{TB}_0 - U^{s}_0]\varepsilon^{s}_{LS}}{\varepsilon^{w}_{TB} - \varepsilon^{s}_{LS}} \tag{17.2}$$

The ΔU_T represents an additional apparent drift. In the particular case of equal distribution parameters ($C^{TB}_0 = C^{s}_0$), Eq. (17.2) reduces to the model used by Van Hout et al. (2002a,b) to explain their data on the TB translation velocity in slug flow. At high U_m, $C^{TB}_0 > C^{s}_0$ is required to represent bubbles overtaking by the rising TB. However, the C^{s}_0 in Eq. (17.2) should characterize the bubble flow in the TB near nose region. The flow phenomena just ahead of the TB nose ($\simeq 1D$) may differ from that in the slug core. In this case, the near TB nose region should form an additional zone in the model (characterized by a different distribution parameter, $C^{n}_0 \neq C^{s}_0$). Equations similar to (9) and (15) can then be used to obtain the gas and liquid velocities and the void fraction in this (third) zone of the slug. However, detailed data, which characterize the different velocity profiles and void fraction in the various regions of aerated slugs, are not yet available. Therefore, the existence of this third zone has not yet been included in the model.

Eq. (17.2) implies that as $\varepsilon^{s}_{LS} \to \varepsilon^{w}_{TB}$, $U_{T\varepsilon} \to \infty$. The liquid slug is then cleavable, and the ordered flow structure is destroyed, leading to churn flow (Jayanti and Brauner, 1995).

2.4. The liquid film velocity

The equations for gas entrainment rate, Φ_{Ge} (Eq. (7.1)) requires the value of the film velocity. The holdup of the film, $\varepsilon_{Lf} = 1 - \varepsilon_{TB}$, and the film average velocity U_{Lf} vary with the distance from the TB nose, $\tilde{z} = z/D$ (see Fig. 1).

The apparent gas flux affected by the moving TB is $U_{BS} = \varepsilon_{TB} U_{GTB}$, and the volumetric flow rate in the adjacent film is obtained from the overall mass balance:

$$U_{LfS} = U_m - U_{BS} = U_m - \varepsilon_{TB} U_{GTB} \tag{18}$$

The local average velocity in the film is related to its local holdup and flow rate:

$$U_{Lf} = \frac{U_{LfS}}{\varepsilon_{Lf}} = \frac{U_{LfS}}{1 - \varepsilon_{TB}} \tag{19}$$

At the TB nose region, the film consists of liquid and gas bubbles. The gas fraction in the liquid film is obtained from a mass balance on the gas, assuming no-slip between the liquid in the film and the gas bubbles, whereby

$$\varepsilon_{GLf} = \frac{\Phi_{GS} - (U_{T\varepsilon} - U_{GTB})\varepsilon_{TB}}{\varepsilon_{Lf}(U_{T\varepsilon} - U_{Lf})}; \quad \varepsilon_{TB} = 1 - \varepsilon_{Lf} \tag{20}$$

and the corresponding mixture density in the film is

$$\rho_f = \rho_L(1 - \varepsilon_{GLf}) + \rho_G \varepsilon_{GLf} \tag{21}$$

The film holdup, ε_{Lf} as a function of the position along the TB, is determined by the momentum balances on the film zone. The momentum balances are performed in a coordinate system moving at the TB translation velocity $U_{T\varepsilon}$, using the one-dimensional approach of the channel flow theory. The derivation of the equations is outlined in Appendix B. Note that, previous derivations in the literature (e.g. Dukler and Hubbard, 1975; Nicholson et al., 1978; Taitel and Barnea, 1990) assumed $U_{T\varepsilon} = U_T$ and an un-aerated film. For film flowing in an annular configuration (as in vertical slug flow), the gradient of the film holdup is given by

$$\frac{d\varepsilon_{Lf}}{d\tilde{z}} = -\frac{d\varepsilon_{TB}}{d\tilde{z}} = -\frac{D(\rho_f - \rho_G)g\sin\beta + \frac{4\tau_f}{\varepsilon_{Lf}} - 4(1-2\tilde{\delta})\left[\frac{1}{\varepsilon_{Lf}} + \frac{1}{1-\varepsilon_{Lf}}\right]\tau_i}{\left[\frac{\rho_f(U_{T\varepsilon}-U_{Lf})(U_{GTB}-U_{Lf})}{\varepsilon_{Lf}} + \frac{\rho_G(U_{T\varepsilon}-U_{GTB})(U_{GTB}-U_{Lf}-\frac{U_{T\varepsilon}}{\varepsilon_{Lf}})}{(1-\varepsilon_{Lf})}\right]} \tag{22.1}$$

with

$$\varepsilon_{Lf} = 1 \quad \text{at } \tilde{z} = 0 \tag{22.2}$$

where

$$\tilde{z} = z/D, \quad \tilde{\delta} = \delta/D \quad \text{and} \quad \varepsilon_{Lf} = 4\tilde{\delta}(1-\tilde{\delta}) = 1 - \varepsilon_{TB} \tag{22.3}$$

For liquid flowing in a trail (a stratified configuration, as in horizontal and inclined slug flow), the dimensionless layer thickness is denoted by $\tilde{h} = h/D$ and the gradient of the film holdup is given by

$$\frac{\mathrm{d}\varepsilon_{\mathrm{Lf}}}{\mathrm{d}\tilde{z}}=\frac{4}{\pi}\widetilde{S}_{\mathrm{i}}\frac{\mathrm{d}\tilde{h}}{\mathrm{d}\tilde{z}}=\frac{4}{\pi}\frac{\frac{\pi}{4}D\Delta\rho g\sin\beta+\frac{\tau_{\mathrm{f}}\widetilde{S}_{\mathrm{f}}}{\varepsilon_{\mathrm{Lf}}}-\frac{\tau_{\mathrm{G}}\widetilde{S}_{\mathrm{G}}}{1-\varepsilon_{\mathrm{Lf}}}-\tau_{\mathrm{i}}\widetilde{S}_{\mathrm{i}}\left(\frac{1}{\varepsilon_{\mathrm{Lf}}}+\frac{1}{1-\varepsilon_{\mathrm{Lf}}}\right)}{\frac{\pi D\Delta\rho g\cos\beta}{4\widetilde{S}_{\mathrm{i}}}-\left[\frac{\rho_{\mathrm{f}}(U_{\mathrm{T}\varepsilon}-U_{\mathrm{Lf}})(U_{\mathrm{GTB}}-U_{\mathrm{Lf}})}{\varepsilon_{\mathrm{Lf}}}+\frac{\rho_{\mathrm{G}}(U_{\mathrm{T}\varepsilon}-U_{\mathrm{GTB}})(U_{\mathrm{GTB}}-U_{\mathrm{Lf}}-\frac{U_{\mathrm{T}\varepsilon}}{\varepsilon_{\mathrm{Lf}}})}{(1-\varepsilon_{\mathrm{Lf}})}\right]} \tag{23.1}$$

with

$$\varepsilon_{\mathrm{Lf}}=\varepsilon_{\mathrm{fc}}\quad\text{at }\tilde{z}=0 \tag{23.2}$$

where

$$\widetilde{S}_{\mathrm{i}}=\sqrt{1-(2\tilde{h}-1)^2}\quad\widetilde{S}_{\mathrm{G}}=\cos^{-1}(2\tilde{h}-1);\quad\widetilde{S}_{\mathrm{f}}=\pi-\widetilde{S}_{\mathrm{G}} \tag{23.3}$$

The value of $\varepsilon_{\mathrm{fc}}$, used as boundary conditions in (23.2), corresponds to the critical film holdup where $\mathrm{d}\varepsilon_{\mathrm{Lf}}/\mathrm{d}\tilde{z}\to\infty$ (i.e., the value of $\varepsilon_{\mathrm{Lf}}$ where the denominator of the r.h.s. of Eq. (23.1) vanishes).

The closure laws for the shear stresses used for carrying out the integration of Eqs. (22) or (23) are (see Appendix B):

$$\begin{aligned}&\tau_{\mathrm{f}}=\tfrac{1}{2}f_{\mathrm{f}}\rho_{\mathrm{L}}U_{\mathrm{Lf}}|U_{\mathrm{Lf}}|;\quad\tau_{\mathrm{G}}=\tfrac{1}{2}f_{\mathrm{G}}\rho_{\mathrm{G}}U_{\mathrm{GTB}}^2\\&\tau_{\mathrm{i}}=\tfrac{1}{2}f_{\mathrm{i}}(U_{\mathrm{GTB}}-U_{\mathrm{Lf}})|U_{\mathrm{GTB}}-U_{\mathrm{Lf}}|\end{aligned} \tag{24}$$

It is worth noting, however, that in most cases the effect of τ_{i} on the film thickness is negligible and practically the same results are obtained with $\tau_{\mathrm{i}}=0$.

Carrying out the integration of Eqs. (22) or of Eqs. (23) up to a prescribed TB length $\widetilde{L}_{\mathrm{TB}}=L_{\mathrm{TB}}/D$ yields the in situ holdup at the TB tail $\varepsilon_{\mathrm{TB}}^{\mathrm{w}}$ and the corresponding velocity in the liquid film:

$$U_{\mathrm{Lf}}^{\mathrm{w}}=\frac{U_{\mathrm{LfS}}^{\mathrm{w}}}{1-\varepsilon_{\mathrm{TB}}^{\mathrm{w}}};\quad\varepsilon_{\mathrm{TB}}^{\mathrm{w}}=1-\varepsilon_{\mathrm{Lf}}^{\mathrm{w}}|_{\tilde{z}=\widetilde{L}_{\mathrm{TB}}} \tag{25}$$

For a long TB, the asymptotic fully developed film thickness $\tilde{\delta}$ (on $\tilde{h}$) corresponds to $\mathrm{d}\varepsilon_{\mathrm{Lf}}/\mathrm{d}\tilde{z}=0$, whereby the numerator of Eqs. (22) (or (23)) equals zero. This provides an algebraic equation for the film thickness.

2.5. The TB and slug lengths

The length of the liquid slug, $\widetilde{L}_{\mathrm{LS}}=L_{\mathrm{LS}}/D$ corresponding to a prescribed $\widetilde{L}_{\mathrm{TB}}$ is obtained from an overall mass balance on the gas phase in a slug unit. For an inlet gas flow rate U_{GS}:

$$U_{\mathrm{GS}}(\widetilde{L}_{\mathrm{TB}}+\widetilde{L}_{\mathrm{LS}})=\int_0^{\widetilde{L}_{\mathrm{TB}}}(\varepsilon_{\mathrm{TB}}U_{\mathrm{GTB}}+\varepsilon_{\mathrm{GLf}}\varepsilon_{\mathrm{Lf}}U_{\mathrm{Lf}})\,\mathrm{d}\tilde{z}+\widetilde{L}_{\mathrm{w}}U_{\mathrm{GLS}}^{\mathrm{w}}\varepsilon_{\mathrm{LS}}^{\mathrm{w}}+(\widetilde{L}_{\mathrm{LS}}-\widetilde{L}_{\mathrm{w}})U_{\mathrm{GLS}}^{\mathrm{s}}\varepsilon_{\mathrm{LS}}^{\mathrm{s}} \tag{26.1}$$

or

$$\widetilde{L}_{\mathrm{LS}}=\frac{U_{\mathrm{GS}}\widetilde{L}_{\mathrm{TB}}-Q_{\mathrm{TB}}-\widetilde{L}_{\mathrm{w}}(U_{\mathrm{GLS}}^{\mathrm{w}}\varepsilon_{\mathrm{LS}}^{\mathrm{w}}-U_{\mathrm{GLS}}^{\mathrm{s}}\varepsilon_{\mathrm{LS}}^{\mathrm{s}})}{U_{\mathrm{GLS}}^{\mathrm{s}}\varepsilon_{\mathrm{LS}}^{\mathrm{s}}-U_{\mathrm{GS}}} \tag{26.2}$$

where $\widetilde{L}_w$ is the length of the TB wake (where $\varepsilon_{LS}^w > \varepsilon_{LS}^s$). The calculations where performed assuming a wake length of 1D. The Q_{TB} in Eq. (26.2) is the gas volume (per unit tube cross section area) carried in the TB. It is obtained by integrating the following differential equation in the range of $0 \leqslant \tilde{z} \leqslant \widetilde{L}_{TB}$:

$$\frac{dQ_{TB}}{d\tilde{z}} = U_{BS} + \varepsilon_{GLf} U_{LfS}; \quad Q_{TB}(\tilde{z}=0) = 0 \tag{27}$$

It is worth noting that a similar overall mass balance on the liquid phase is redundant, since it is already satisfied by the mass balances in Eqs. (8) and (18).

3. Solution procedure and parameters

For a fully developed liquid film corresponding to $L_{TB} \to \infty$ (and $L_{LS} \to \infty$), the model requires a solution of four non-linear algebraic equations (NLE system) for the unknowns $\tilde{h}$ (or $\tilde{\delta}$), $U_{T\varepsilon}$, ε_{LS}^w and ε_{LS}^s. The four equations are the numerator of Eqs. (22) (or (23)), (17.1), (15.1), (15.2) (all written as implicit equations with zero on their r.h.s.). The other model equations are explicit auxiliary equations that are needed for solving these four implicit equations. The solution so obtained yields the asymptotic values of the film thickness and velocity, δ^∞ (or h^∞) and U_{Lf}^∞, the maximal gas entrainment rate Φ_{GS}^∞, the maximal TB translation velocity $U_{T\varepsilon}^\infty$ and the in situ gas fraction in the slug $(\varepsilon_{LS}^w)^\infty$, $(\varepsilon_{LS}^s)^\infty$. This NLE system has been solved using the POLYMATH software package (Shacham and Cutlip, 1996).

In the case of a finite length Taylor bubble, the model requires integration of the differential equation (22) (or (23)) for the film thickness up to a specified length $\tilde{z} = \widetilde{L}_{TB}$. Since the unknown gas entrainment rate and the slug translation velocity $(U_{T\varepsilon})$ are dependent on the condition at the TB tail $(\tilde{z} = \widetilde{L}_{TB})$, it is a boundary value problem. For a short TB, for which $We < We_c$ (see Eqs. (7)), gas is not entrained into the slug, hence $U_{T\varepsilon} = U_T$ (Eq. (10)). Thus, the integration of Eqs. (22) (or (23)) with $U_{T\varepsilon} = U_T$ and $\Phi_{GS} = 0$ is valid only for TB shorter than a critical length, corresponding to the onset of gas entrainment. For a longer TB, a value $U_T < U_{T\varepsilon} < U_{T\varepsilon}^\infty$ corresponds to a certain bubble length L_{TB}. Since the integration of Eqs. (22) (or (23)) up to a specified $\widetilde{L}_{TB}$ requires a tedious iteration procedure, it is easier to carry out the calculation in two stages according to the following procedure.

At the first stage, the momentum equation (22) (or (23)) is replaced by a prescribed value of liquid film holdup at the bubble tail, ε_{Lf}^w. The prescribed value should be in the range $\varepsilon_{Lf}^w(\tilde{z} \to \infty) < \varepsilon_{Lf}^w < \varepsilon_{Lf}(\tilde{z}=0)$. The remaining three implicit algebraic equations ((17.1), (15.1) and (15.2)) are then solved to obtain $U_{T\varepsilon}$, ε_{LS}^w, ε_{LS}^s and the Φ_{GS} by Eq. (16). In the second stage, the corresponding TB and slug lengths are obtained by integrating Eqs. (22) (or Eqs. (23)) up to the prescribed value, ε_{Lf}^w (using the value already obtained for $U_{T\varepsilon}$ and other required information as input). The ordinary differential equation (ODE) system has been solved using MATLAB.

The application of the drift-flux model in the framework of the TBW model requires assigning values for the distribution parameters C_0^{TB}, and C_0^w and C_0^s. The value of C_0^{TB} depends on the velocity profile ahead of the TB nose. This dependence was confirmed by theoretical and experimental studies, which were reviewed by Fabre and Liné (1992). In vertical systems and unaerated slugs, the theory suggests $C_0^{TB} = 2.27$ for laminar flow and $C_0^{TB} = 1.2$–1.4 for turbulent

flow (Collins et al., 1978). These values are close to the ratio of the maximum to mean velocity of the liquid in the slug. Hence, values that are commonly used to model the TB rise velocity are $C_0^{TB} \approx 2$, 1.2 in laminar and turbulent flows, respectively. There are some evidences that in horizontal and inclined systems the C_0^{TB} values are lower (Bendiksen, 1984; Van Hout et al., 2002a,b). Also, in low Eo_D systems, surface tension affects a reduction of C_0^{TB} (Bendiksen, 1985). Moreover, measurements in bubbly flow indicate that the bubbles tend to flatten the velocity profile (Hibiki and Ishii, 1999). Therefore, lower values of C_0^{TB} may be required to model the TB motion in aerated slug flow compared to those obtained with pure liquid slugs.

If a uniform bubble distribution across the pipe can characterize the TB near and far wake regions in the slug, then $C_0^w, C_0^s = 1$. Otherwise, their rigorous computation requires the bubble and velocity distributions in these regions, which are yet unavailable. However, wall peaking in void fraction distribution generally results in $C_0 < 1$, whereas $C_0 > 1$ characterizes center peaking. The latter is believed to be more relevant in case of adiabatic vertical upward slug flow. The sensitivity of C_0 to variations in the velocity and void fraction profiles was studied in the literature (e.g. Zuber and Findley, 1965; Hibiki and Ishii, 2002). Typical axisymmetric power-law profiles yields $1.05 < C_0 < 1.3$, the higher values correspond to a more pronounced center peaking of the velocity and void fraction distributions. Experimental studies in vertical bubbly flow indicate that void fraction profiles are affected by several factors, including the tube inclination, mixture velocity, bubble size distribution and average void fraction (Hibiki and Ishii, 2002). In inclined and horizontal flows the evaluation of C_0 is even more complicated, since the bubble concentration and velocity profiles are not necessarily axisymmetric.

The results presented in the next section were obtained with values of C_0^w, $C_0^s = 1$–1.2 corresponding to flat or center peaked bubble concentration profiles. Some parametric studies were carried out to examine the sensitivity of the model prediction to variations in the assumed distribution parameters C_0^w, C_0^s and C_0^{TB}.

4. The TBW model predictions

4.1. Vertical slug flow

Fig. 2 shows the void fraction in the slug predicted by the TBW model for vertical upward air–water flow. The calculated values are for a fully developed liquid film, which is reached asymptotically for sufficiently long TB. Note that, in vertical slug flow and moderate mixture velocities, the fully developed film flow is practically approached for a TB length of about $20D$. Uniform bubble distribution are assumed in the TB near and far wake regions ($C_0^w = C_0^s = 1$), while $C_0^{TB} = 1.2$.

The bold curve shows the results obtained without back-flow, since for $D > 5$ cm, $U_0^{TB} > U_0^w$ and the back-flow is suppressed even in the limit of $U_m \to 0$. Since the same distribution coefficient is used for the TB near and far wake regions, $\varepsilon_{LS}^w = \varepsilon_{LS}^s (= \varepsilon_{LS})$ is predicted. The dashed curves show the results when the back-flow of the entrained bubbles is nevertheless included, assuming for the moment that for the bubbles entrained in the TB wake, the velocity relative to the TB tail is their drift velocity. In this case the back-flow (Eq. (13)) is proportional to U_0^w, and lower ε_{LS} is obtained. As shown in Fig. 2, this back-flow has a significant effect only for low mixture

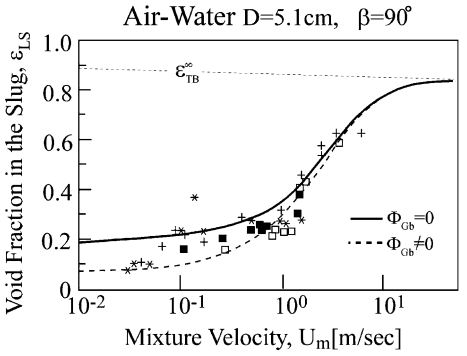

Fig. 2. The TBW model prediction for the asymptotic void fraction in the slug obtained with long TB ($L_{TB} \to \infty$), with and without back-flow (Φ_{Gb}) in a vertical air–water system. Bubbles distribution parameters $C_0^{TB} = 1.2$, $C_0^w = C_0^s = 1$, $\varepsilon^{\infty}_{TB}$ is the TB void fraction. Experimental data: + Barnea and Shemer (1989), * Fernandes (1981), □ Mao and Dukler (1989), ■ Van Hout et al. (1992).

velocities. With increasing U_m, practically the same values are predicted with and without back-flow.

The comparison of the model predictions with data shown in Fig. 2 is favorable. In particular, the TBW model predictions follow the trend of the steep increase of ε_{LS} for $U_m > 1.5$ m/s. In agreement with the experimental data, the model predicts that as $U_m \to 0$, the slug void fraction levels off at a value of $\varepsilon_{LS} \simeq 0.15$–$0.2$. It is worth noting that according to the TBW model, the value of ε_{LS} at high U_m approaches the value of the TB void fraction, ε^w_{TB}, only asymptotically. However, the difference between ε_{LS} and ε^w_{TB} becomes negligible for $U_m > 10$ m/s. This implies a collapse of the slug bridges and transition to churning or annular flow is expected in the system.

The appearance of a relatively high void fraction region at the TB wake have been commonly attributed to the bubble back-flow. However, the velocity profile in the wake is highly distorted due to the plunging liquid film and extremely center peaked (Van Hout et al., 2002a,b). Hence a larger value of the distribution parameter in the near wake region may be required to adequately characterize the different gas velocity in the TB near and far wake regions. In view of Eqs. (8.1), (9.1) and (15), a value of $C_0^w > C_0^s$ results in $\varepsilon^w_{LS} > \varepsilon^s_{LS}$ (irrespective of the back-flow rate).

The consequences of using $C_0^w > C_0^s$ on the predicted void fraction in the slug are shown in Fig. 3a (back-flow is suppressed). Obviously in the range of low mixture velocities, where the gas velocity in the slug is determined by the bubble drift velocity, the results are insensitive to the value of C_0^w. However, using a higher value for C_0^w has a pronounced effect on the void fraction in the slug core at high mixture velocities. While the values of ε^w_{LS} are almost unaffected by the change of C_0^w also at high mixture velocities (see Figs. 2 and 3a), the values of ε^s_{LS} are lower. The difference between ε^w_{LS} and ε^s_{LS} increases with U_m and saturates at about $\Delta\varepsilon_{LS} = \varepsilon^w_{LS} - \varepsilon^s_{LS} \simeq 0.3$ at high U_m. The data in this region, which represents average values over the slug unit, are in-between the predictions of ε^w_{LS} and ε^s_{LS} obtained with $C_0^w > C_0^s$. It is worth noting, however, that if the value of C_0^s is also set to $1.2(= C_0^w)$, $\varepsilon^s_{LS} = \varepsilon^w_{LS}$ is obtained again, and their values are almost the same as those obtained with $C_0^w = C_0^s = 1$ (see Fig. 3b). In fact, the predicted void fraction in the slug is insensitive to the values of these distribution parameters, as long as the same values are used to

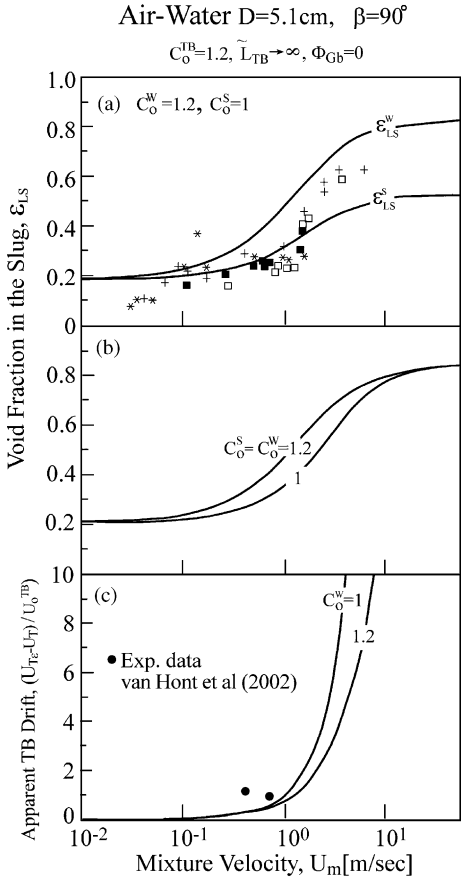

Fig. 3. Effect of the drift-flux model parameters on the asymptotic void fraction and TB translation velocity in air–water vertical flow (data notation as in Fig. 2).

characterize the TB near and far wake regions. Therefore, the comparison with the data of ε_{LS} (Fig. 3a) does not provide a clue on the appropriate value for C_0^w and C_0^s.

The predicted TB translation velocity is shown in Fig. 3c. The recurrent bubble coalescence at the TB nose and their re-entrainment at the TB tail affect an apparent higher TB drift velocity (see Eqs. (17)). The apparent drift increases with the slug void fraction, hence with the mixture velocity. Fig. 3c shows that the increased drift is almost indistinguishable at low mixture velocities. However, it increases dramatically at $U_m > 1$ m/s following the trend of the steep increase in the slug void fraction. This increase is attenuated when a value of $C_0^w > 1$ is used. Recent data of Van Hout et al. (2002a,b) confirm the increase of the TB translation velocity due to slug aeration.

It is of interest in this respect to refer to the data of Cheng et al. (1998) for the propagation velocity of void fraction waves taken in vertical upward air–water flow in a 15 cm diameter pipe. Although they did not detect transition to slug flow, but a rather gradual transition from bubble flow to churn flow, they attempted to compare their data with Nicklin et al. (1962) model (Eq. (10) with $C_0^{TB} = 1.2$) and with other models from the literature. All were found to significantly un-

derpredict the measured velocities. The data imply an increased drift compared to the Nicklin et al. (1962) model. Their data are shown in Fig. 4 in comparison with the TB translation velocity predicted by the TBW model. Fig. 4b shows that the increased apparent drift is already of the order of U_0^{TB} at low mixture velocities and becomes several times higher than U_0^{TB} at high U_m. Consequently the slope of $U_{T\varepsilon}$ vs. U_m curve appears to be steeper than 1.2, which is the value used in the Nicklin et al. (1962) model ($U_N^T = 1.2U_m + U_0^{TB}$). It is therefore important to realize that the apparent drift due to the bubble entrainment/coalescence process cannot be deduced from the intercept of the $U_{T\varepsilon}$ vs. U_m curve at $U_m \to 0$. The TB distribution parameter cannot be deduced from the slope of the curve either. The values predicted for the void fraction in the slug for this system are shown in Fig. 4c. The difference between the void fraction values obtained with the various C_0^{TB} and C_0^w is indistinguishable in the figure scales.

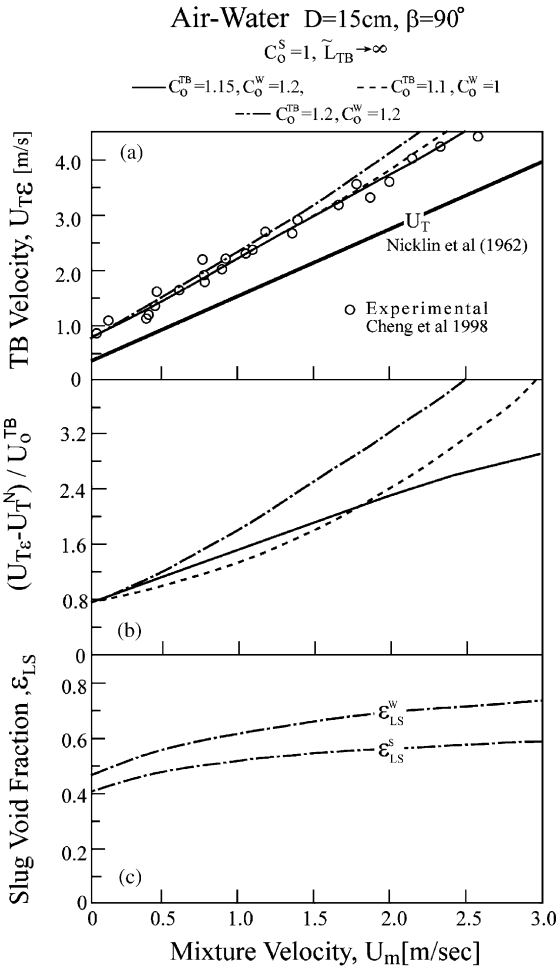

Fig. 4. The TBW model predictions for a vertical air–water 15 cm tube—comparison of the TB translation velocity with experimental data of void fraction waves obtained by Cheng et al. (1998).

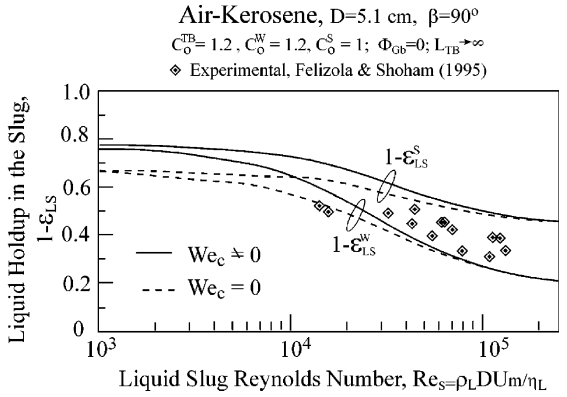

Fig. 5. Comparison of the TBW model prediction for the asymptotic slug void fraction with experimental data taken in a vertical air–kerosene system of Felizola and Shoham (1995).

In Fig. 5 the TBW model results for an air–kerosene system are tested against the data of Felizola and Shoham (1995) using their scales. It is worth noting that the gas entrainment rate is predicted to increase proportionally to $\sigma^{-1/2}$ (see Eqs. (7)). Indeed, for the lower surface tension of air–kerosene ($\sigma = 28$ dyne/cm), the slug aeration is somewhat higher than in air–water slug flow (Fig. 2a). The change is more pronounced at low U_m (low Re_s), whereas at high U_m it is almost insignificant for this surface tension difference. At very high U_m, where $\varepsilon^s_{LS} \to \varepsilon^w_{TB}$ is predicted, the surface tension effect is negligible. This may be the reason for the apparent low sensitivity to surface tension implied by data of slug void fraction obtained in various gas–liquid systems.

Another point which is evident in view of Fig. 5 is that the effect of a threshold value of the Weber number for onset of bubbles entrainment (We_c in Eqs. (7)) is significant only in the range of relatively low U_m. The lower the critical Weber number is, the higher is the value of ε_{LS} at low mixture velocities. In the range of high mixture velocities, the results obtained with $We_c \neq 0$ or $We_c = 0$ are practically the same. Since no back-flow is predicted ($\Phi_{Gb} = 0$), $\varepsilon^w_{LS} = \varepsilon^s_{LS}$ is obtained at low Re_s (low U_m). However, at higher Re_s the TB wake is predicted to be more aerated due to $C^w_0 > C^s_0$. The data representing averaged values are shown to be in the range between ε^w_{LS} and ε^s_{LS}. It is worth recalling, however, that the results shown in Figs. 3–5 are for a fully developed liquid film ($L_{TB} \to \infty$). These asymptotic values provide the upper limit on slug aeration. Lower values for ε^w_{LS} and ε^s_{LS} result with the finite TB lengths observed in real systems. This issue will be further discussed below.

An important parameter of slug flow models is the distribution parameter for the TB rise velocity (C^{TB}_0 in Eq. (10)). In the case of un-aerated liquid slugs, it has been established in the literature that its value depends on the velocity profile in the liquid ahead of the TB nose, and the value of $C^{TB}_0 \simeq 1.2$ and $C^{TB}_0 \simeq 2$ are commonly used for turbulent and laminar flow respectively. However, the value of C^{TB}_0 was reported to be dependent also on the tube inclination, Eötvös number and Froude number, $Fr = U_m/[\frac{\Delta\rho}{\rho_L} g]^{0.5}$ (e.g. Fabre and Liné, 1992). The ambiguity concerning the value of C^{TB}_0 becomes even more problematic in the case of a TB rising through an aerated liquid slug. This happens since the slope of a curve depicting the TB experimental translation velocity vs. U_m (used to deduce C^{TB}_0) is affected by the increased apparent drift due to

the bubble coalescense/entrainment phenomena. As discussed above, the latter is dependent on the mixture velocity. Therefore, it is of interest here to assess the sensitivity of the model prediction to the value taken for C_0^{TB}.

Fig. 6a shows the results obtained for the slug void fraction in the case of vertical air–water slug flow with values of C_0^{TB} varies in the range of 1–1.2 ($C_0^w = C_0^s = 1$, therefore, $\varepsilon_{LS}^s = \varepsilon_{LS}^w = \varepsilon_{LS}$). At the low U_m range ($U_m < 0.04$ m/s), where the flow in the slug is laminar, larger C_0^{TB} may have to be considered. However, as shown in the figure the values of the void fraction are practically insensitive to C_0^{TB}. A slight increase of ε_{LS} with increasing C_0^{TB} results only in the range of extremely high U_m, where slug flow may not exist. Obviously, the value of C_0^{TB} affects the TB rise velocity at high U_m. Fig. 6b shows the increase of the TB translation velocity compared to that expected by the Nicklin et al. (1962) model, U_T^N. The increase of $U_{T\varepsilon}$ with U_m is very much attenuated as C_0^{TB} is reduced. In light of Hibiki and Ishii findings (1999), it is possible that aerated slugs are characterized by flatter velocity profiles (in the TB far wake region) compared to unaerated slugs. In this case values of $C_0^{TB} < 1.2$ may be appropriate at high mixture velocities. As

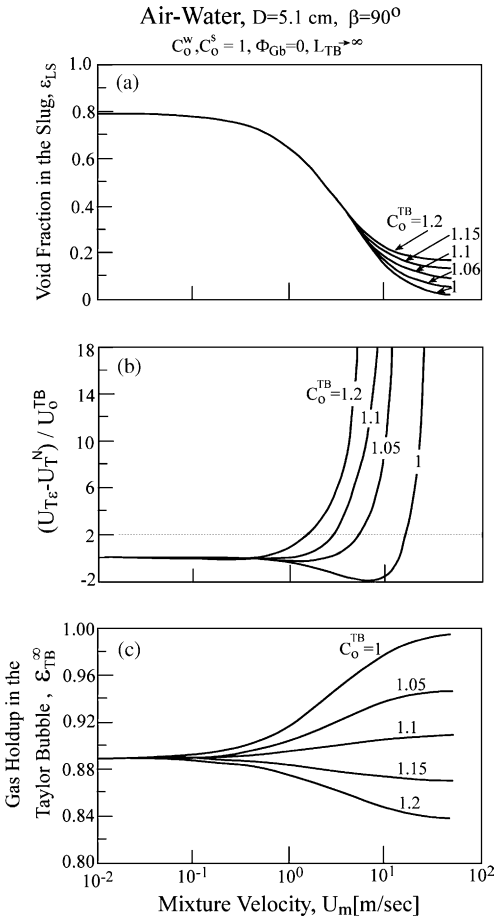

Fig. 6. Effect of the TB distribution parameter on the TBW model predictions for a vertical air–water system.

shown in Fig. 6b, the combined opposing effects of a lower C_0^{TB} and high apparent drift (due to the bubble entrainment/coalescence process) extend the range of mixture velocities where the Nicklin et al. (1962) model adequately represents $U_{T\varepsilon}$. Moreover, in the case of a flat velocity profile at the TB nose ($C_0^{TB} = 1$), the Nicklin model may even overpredict the TB translation velocity for some intermediate range of mixture velocities. As shown in Fig. 6c, a change of C_0^{TB} has also a very pronounced effect on the value of ε_{TB} (or ε_{Lf}). As U_m is increased, even the trend of ε_{TB} vs. U_m changes with $C_0^{TB} < 1.1$. The sensitivity of the liquid film thickness to the variation of C_0^{TB} suggests that measurements of liquid film thickness (for long TB's) can provide an indication on the appropriate value of C_0^{TB}. It is worth recalling that for vertical slug flow the TBW model have been applied with $C_0^{TB} \simeq 1.2$ (Figs. 2–5).

4.2. Inclined slug flow

The data available in the literature on the liquid slug void fraction in inclined flows are limited. Nuland et al. (1997), however, provided a well documented data on the various slug characteristics obtained in an oil–dense gas system. The data included the slug and TB void fraction, the average void fraction, the slug front translation velocity and the corresponding oil and gas flow rates for 10°, 20°, 45° and 60° (4–6 points at each) inclination. In order to compare the TBW model predictions with their data, the average length of the liquid slug is taken as $22D$, which is considered a representative value for fully developed slug flow in horizontal and inclined systems (e.g. Felizola and Shoham, 1995). The corresponding TB length as a function of the operational conditions evolves from the overall mass balance (Eqs. (26)). The procedure followed for estimating the distribution parameters for the TBW model is described in Appendix C. The results shown in Fig. 7 were obtained with $C_0^{TB} = 1.1, 1.05, 1, 0.95$ at $\beta = 10°, 20°, 45°, 60°$ respectively, and $C_0^w = C_0^s = 1.15$ at all inclinations.

A comparison between the predicted and experimental values of the void fraction in the slug is shown in Fig. 7a. Note that, since the back-flow has practically no effect in this large diameter tube ($D = 10$ cm), and since $C_0^w = C_0^s$ is used, the predicted ε_{LS} corresponds to $\varepsilon_{LS}^s = \varepsilon_{LS}^w$. The favorable comparison indicates that the TBW model is capable of predicting the effect of the mixture velocity, liquid-cut in the feed and inclination on the slug void fraction. In particular, the high values of ε_{LS} obtained at 60° inclination are well predicted by the model. It is worth emphasizing that the value of ε_{LS} increases not only with the mixture velocity, but also with the gas-cut in the feed. Lower gas-cut (U_{GS}/U_m) in the feed results in a shorter TB for a specified average slug length. A shorter TB is associated with a lower film velocity, and consequently with a lower rate of gas entrainment into the slug. The corresponding TB-to-slug length ratio is shown in Fig. 7d vs. the gas-cut in the feed. As expected, for a constant β, higher gas-cut is associated with a longer TB. This figure also shows that the typical TB becomes longer as the inclination is reduced. As shown in Appendix C (Fig. 16d) values of ε_{LS} associated with fully developed film flow ($L_{TB} \to \infty$) overestimate the experimental data. This indicates that, in general, a fully developed film flow cannot be assumed for the TB lengths that satisfy the overall mass balance, Eq. (27), with the typical slug length of $L_{LS} = 22D$.

As already discussed with reference to previous figures, variations in the values used for the distribution parameters have a minor effect on the average ε_{LS}. Indeed the comparison between the predicted ε_{LS} and the data shown in Fig. 7a is similar to that obtained assuming uniform

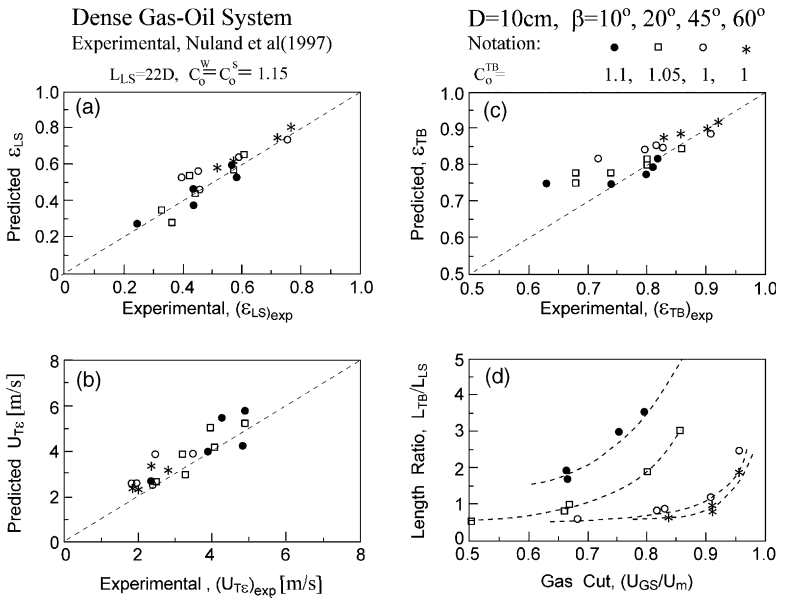

Fig. 7. The TBW model prediction for an inclined dense gas–oil system with C_0^{TB} tuned—comparison with experimental data of Nuland et al. (1997).

bubble distributions in the TB near and far wake regions (see Appendix C, Fig. 16c). The values assigned to the distribution parameters should be more carefully considered in order to correctly predict the TB translation velocity and its void fraction. Indeed, Fig. 7b and c indicate a reasonable comparison also with the data for $U_{T\varepsilon}$ and ε_{TB}.

The model explains that a variability of ε_{LS} can be expected even when all operational conditions are maintained constant, due to variability of the TB length (and the slug length) as commonly observed in slug flow. The variability of the TB length is associated with a variability in the ε_{TB}^{w} and U_{Lf}^{w} hence, in the gas entrainment rate at the TB tail. This, in turn, results in a variability of the gas fraction in the slug, and in the TB translation velocity, $U_{T\varepsilon}$. Any value of ε_{LS} in the range of $0 \leqslant \varepsilon_{LS} \leqslant \varepsilon_{LS}^{\infty}(L_{TB} \to \infty)$ actually corresponds to a specific value of $\varepsilon_{TB}^{w} \leqslant \varepsilon_{TB}^{\infty}$ and a corresponding $U_{T\varepsilon}$ in the range of $U_T \leqslant U_{T\varepsilon} \leqslant U_{T\varepsilon}^{\infty}$.

The variation of ε_{LS} with the TB length is further demonstrated in Fig. 8 in comparison with the data of Felizola and Shoham (1995) (as shown in Gomez et al., 2000) for upward inclination of $\beta = 50°$. The predicted ε_{LS} increases with Re_s (or U_m) and with the TB length. The comparison with the data implies L_{TB} of about 10–15D in the range of relatively low Re_s, and an increase of L_{TB} with Re_s. The kerosene and air flow rates corresponding to these data points were not specified. However, in general, high U_m in slug flow corresponds to high gas-cut, hence longer TB.

The effect of inclination as represented by the model is demonstrated in Fig. 9 with reference to the kerosene–air system studied in Fig. 8. Fig. 9a shows the variation of the liquid holdup in the slug as the tube inclination is increased from the horizontal to the vertical position for two mixture velocities and a constant liquid-cut in the feed (20%). It is to be noted that although the comparison with the data of Nuland et al. (1997) implies the distribution parameters (e.g. C_0^{TB}) vary with the inclination, their effect on the average slug void fraction was shown to be rather

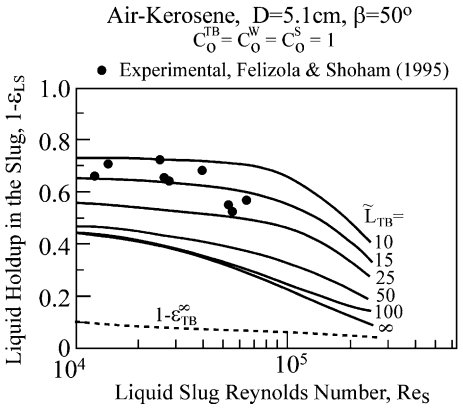

Fig. 8. Effect of TB length on the predicted slug holdup in 50° inclined air–kerosene system—comparison with experimental data of Felizola and Shoham (1995).

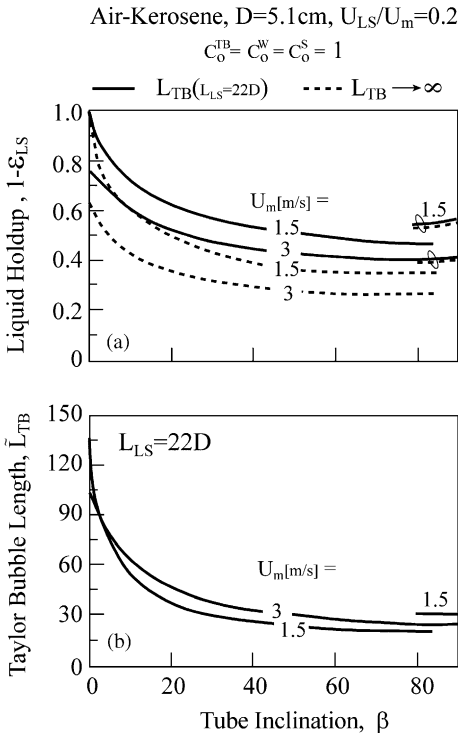

Fig. 9. Effect of the inclination on the TBW model prediction.

mild. Therefore, the effect of inclination on ε_{LS} is demonstrated by applying the model with constant values of these parameters, C_0^{TB}, C_0^w, $C_0^s = 1$. The bold lines in Fig. 9a shows the slug holdup corresponding to TB length associated with $L_{LS} = 22D$, whereas the dashed lines indicate the asymptotic values that would have been obtained if the slug is preceded by a long TB with a

fully developed liquid film. The figure shows that for a constant liquid-cut and mixture velocity, the model indicates a monotonous decrease of the liquid holdup in the slug with increasing the inclination. This trend is at least with qualitative agreement with the data of Felizola and Shoham (1995). The higher void fraction in the slug at steeper upward inclinations results in shorter TBs that satisfy the overall mass balance for the specified slug length ($L_{LS} = 22D$, Fig. 9b). Note that the figure implies a discontinuous switch at steep inclinations (except for $U_m = 3$ m/s and $L_{LS} = 22D$, where it appears continuous). This switch results from the different models used for vertical (and slight off-vertical) upflows and inclined flows. While for the former an annular configuration in the TB region is appropriate, in inclined flows the stratified configuration is assumed. This discontinuity is obviously an artifact of the different models (applied with the same value for C_0^{TB} and C_0^{w}), whereas in reality a smooth transition is expected.

A more elaborate evaluation of the effect of inclination on the averaged values of the slug holdup requires consideration of the variation of the distribution parameters and the typical slug length with the inclination. Felizola and Shoham (1995) reported a variation of the average slug length with the inclination. Although $L_{LS} \simeq 22D$ is in the range of the standard deviation of the slug length distribution obtained at all inclinations, the average L_{LS} indicate a minimum value of $L_{LS} \simeq 16D$ at $\beta \simeq 60°$.

4.3. Horizontal slug flow

Having demonstrated the TBW model as a predictive tool for vertical and inclined slug flow, it is of interest to test its applicability to horizontal flow. The main difference between horizontal and upward inclined flows, is the velocity in the liquid film. Due to the gravity, in inclined flows the liquid in the film is draining backwards, flowing countercurrently to the liquid in the slug. The steeper the inclination is, the higher is the backward velocity in the film, and in vertical pipes it is much higher than the upward liquid velocity in the slug. Whereas in horizontal slug flow, the liquid in the slug front flows concurrently to the liquid in the film overtaking the almost immobile liquid in the film. Also, in view of Eqs. (8.3) and (13), bubble back-flow is even less likely ($\Phi_{Gb} = 0$).

Fig. 10 shows the results of the TBW model when applied to the air–oil system used by Gregory et al. (1978) in $D = 5.12$ cm pipes. It is worth noting that for this system, the critical Weber number suggested in Eqs. (7) implies a threshold value on the mixture velocity of $U_m \simeq 1.5$ m/s below which un-aerated slug flow is predicted. Note also that practically, the same threshold value is indicated by the $(U_m)_{crit}$ of the SLB model (Table 1). However, the data of Gregory et al. (1978) indicate minute values of $\varepsilon_{LS} > 0$ for lower mixture velocities and a better overall prediction of the TBW is obtained at low U_m with $We_c = 0$.

As in vertical and inclined flows, the effect of the TB length becomes more pronounced as the mixture velocity is increased and longer TBs are required for approaching the maximal asymptotic void fraction. This is implied also by the data that become very scattered for high mixture velocities. In real slug flow, the TB length is non-unique even when the input flow rates are maintained constant. Moreover, as have been already discussed with reference to Fig. 7d, high liquid-cut in the feed results in relatively short TB. In this case, the model predicts higher liquid holdups in the slugs compared to those obtained for the same mixture velocity, but with a lower liquid-cut, where the TB length distribution is shifted towards higher values. Thus, inherent

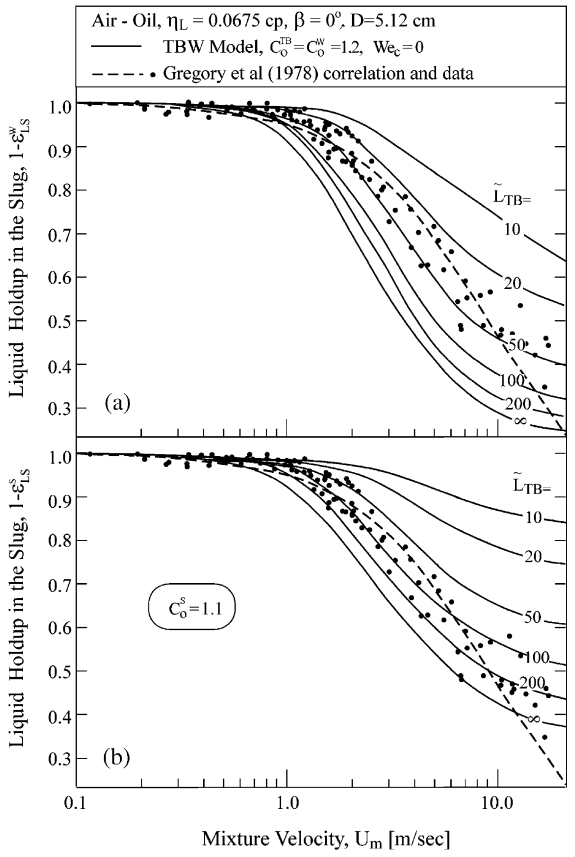

Fig. 10. Effect of TB length on the predicted slug holdup in horizontal oil–air flow—comparison with Gregory et al. (1978) data and correlation.

scattering is expected when data of slug holdup are depicted vs. the mixture velocity. This is further demonstrated in Fig. 11, where the model predictions for 50% and 10% oil-cut in the feed and slug length of 30D are compared with the data of Zheng (1991). The oil-cuts are in accordance with the experimental range and the 30D slug length corresponds to the peak value of the reported slug length distribution. As shown in the figure, the data for the slug holdup obtained with various oil-cuts are in the range of the predictions obtained for high and low oil-cut. Note that, given the oil-cut in the feed, a minimal TB length is required for satisfying the overall mass balance (Eqs. (26)). The minimal TB length increases with the gas-cut. For the lowest gas-cut of 50%, and a shortest slug bridge of $L_{LS} \approx D$, the $(L_{TB})_{min}$ is already of about 30D. As shown in Fig. 11, the liquid holdup associated with the shorter TB (dashed line) is higher than the values obtained with the TB associated with $L_{LS} = 30D$.

The predicted values of ε_{LS} in Fig. 10a correspond to the holdup in the slug front if the model is applied with $C_0^s < C_0^w$, or to $\varepsilon_{LS}^s = \varepsilon_{LS}^w$ if $C_0^s = C_0^w (= 1.2)$. The variation of ε_{LS}^s if $C_0^w > C_0^s (= 1.1)$ is used, are shown in Fig. 10b. Similarly to the results obtained in vertical (and inclined) flows, $\varepsilon_{LS}^s < \varepsilon_{LS}^w$ is predicted in this case, whereby the slug front region appears more aerated than the

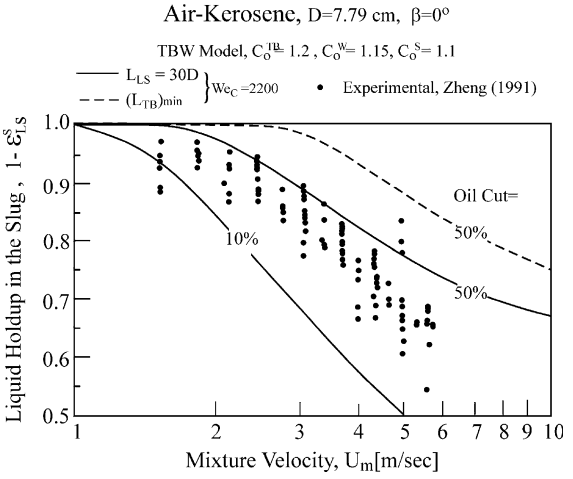

Fig. 11. Effect of the water-cut in the feed in horizontal flow on the predicted holdup in slugs—comparison with the data of Zheng (1991).

slug core region. Longer TBs are implied by the results in Fig. 10b as to match the measured values.

The effects of the TB length and mixture velocity on the TB translation velocity are shown in Fig. 12a. For low U_m, where the gas entrained into the slug is minute, the TB translation velocity is identical to that obtained by the Nicklin et al. (1962) equation. However, as the rate of gas entrainment increases due to higher mixture velocities and/or longer TB, the apparent TB drift and the effective TB translation velocity increase. For the TBW model parameters used in Fig. 10 and long TBs, the apparent drift is 3–5 times the TB drift, U_0^{TB}.

The fact that in horizontal (and slightly downward inclined) slug flows the bubble entrainment is dominated by the liquid velocity in the slug, rather than by the film velocity, explains why the SLB model, which is based on Barnea and Brauner (1985) approach (Table 1), yields favorable results in these systems. As in the SLB model, the mixture velocity in the TBW model actually represents the characteristic velocity for bubble entrainment. Hence, both models suggest the same Weber number and Eötvös number as controlling dimensionless variables. However, combining Eqs. (7), (15) and (17), it can be shown that for low Φ_{Ge} (relatively low U_m), the TBW model suggests also the Froude number, $U_m \Big/ \sqrt{\frac{\Delta\rho}{\rho_L} gD}$ as a controlling dimensionless parameters, whereby $\varepsilon_{LS}^{s} \propto Eo_D^{-1/2} WeFr$.

4.4. Effect of tube diameter

From the practical point of view, the effect of tube diameter on the slug void fraction is of particular interest for up-scaling laboratory data to larger diameters encountered in field operations. Gregory et al. (1978) measured the slug void fraction also in a 2.58 cm pipe. The effect of tube diameter indicated in their data is modest and inconsistent; ε_{LS} tending to slightly higher values at low mixture velocities for the 2.58 cm pipe and slightly lower values at high mixture velocities. In view of the scattering of the data, their correlation suggests no diameter effect. Fig.

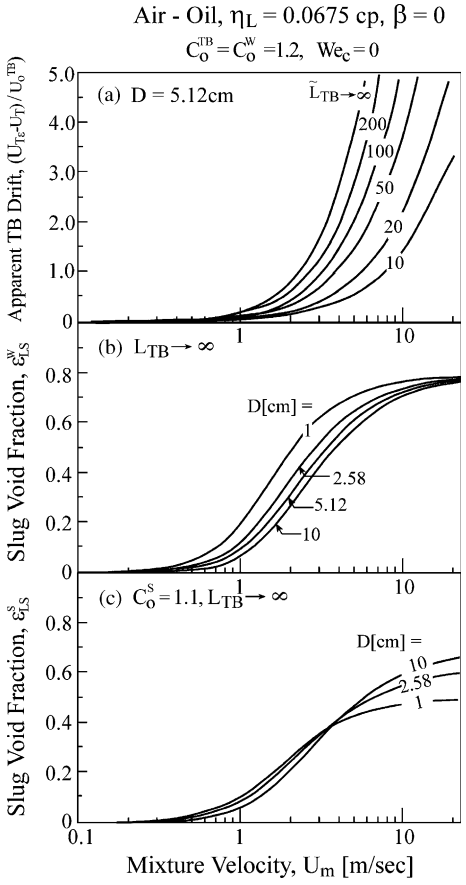

Fig. 12. Horizontal oil–air system: (a) effect of the TB length on the TB translation velocity compared to Nicklin model, U_T^N; (b) effect of D on the asymptotic ε_{LS}^w in the TB wake, $\varepsilon_{LS}^s = \varepsilon_{LS}^w$ in case $C_0^s = 1.2$ is used; (c) effect of D on the asymptotic ε_{LS}^s with $C_0^s = 1.1$.

12b and c shows the variation of the asymptotic values of ε_{LS} with the tube diameter as predicted by the TBW model. Indeed, the effect of tube diameter is predicted to be very modest, and is expected to be overshadowed by the effects of other parameters of the slug flow (such as slug length distribution) which have been found to have much more pronounced effects.

The modest variation of ε_{LS}^w with the tube diameter is due to the change in the TB drift velocity. Increasing D results in higher U_0^{TB}, hence, higher TB rise velocity (Eq. (12)). This in turn results in a lower ε_{TB}^w, and higher (positive) U_{Lf}. However, in horizontal flow, the bubble entrainment is due to $U_{LLS}^w \gg U_{Lf}$. Therefore, variation of U_{Lf} has almost no effect on the rate of gas entrainment (Φ_{Ge}) and the associated ε_{LS}^w. For $\varepsilon_{LS}^s < \varepsilon_{LS}^w$ (Fig. 12c) the trend of variation with D can even be reversed at high U_m. This is due to the fact that the difference between ε_{LS}^s and ε_{LS}^w becomes significant at high U_m and increases with reducing the pipe diameter. Consequently, as shown in Fig. 12c, the net effect of D on ε_{LS}^s at high U_m is opposite to that obtained at low U_m. It is of interest to note that these trends of variations of ε_{LS}^s with D and U_m are consistent with the findings of Gregory et al. (1978).

Consistent with Fig. 10 the results shown in Fig. 12 assume $We_c = 0$. With $We_c \neq 0$, $\varepsilon^s_{LS} \equiv 0$ is obtained for $U_m \sim< 1.5$ m/s. In view of Eqs. (7), in large Eo_D systems, this threshold value is practically independent of D in horizontal slug flow and long TBs, where the velocity difference between the slug and the film is dominated by U^w_{LLS}.

The effect of the tube diameter on the slug void fraction is much more pronounced in vertical and steeply inclined tubes. This is demonstrated in Fig. 13, where the variation of ε_{LS} with D at constant U_m is shown for air–water vertical upward slug flow. Note that the dimensional (logarithmic) scale of D is used for the sake of convenient interpretation, and the corresponding dimensionless Eo_D scale is also indicated. In vertical slug flow, the velocity difference between the film and the slug is dominated by the film (downward) velocity. Therefore here, the increase of the film velocity with increasing D, results in a higher rate of bubble entrainment at the TB tail, hence higher ε^w_{LS} and ε^s_{LS}. Moreover, with $We_c \neq 0$, the critical mixture velocity for the onset of bubble entrainment is dependent on D. As shown in Fig. 13, a larger D is associated with a lower threshold value for U_m for the onset of entrainment. The decline of slug void fraction with reducing D (at constant U_m) becomes steeper as the Weber number approaches the critical value.

It is worth noting that for $Eo_D < 5$, the variation of ε_{LS} with D is affected also by the decrease of C^{TB}_v with Eo_D (see Eqs. (11) and Appendix A). However, this variation becomes relevant only for high U_m, since at $U_m < 1.5$ m/s, the smallest D for obtaining aerated slug already corresponds to $Eo_D > 5$.

The relevance of the results shown in Fig. 13 are not limited to vertical slug flow. In small tubes of low Eo_D, the role of gravity diminishes and capillary forces become important. Consequently, depending on the liquid wall wettability, the annular configuration can be obtained in the TB region even in horizontal flows (Brauner et al., 1996, 1998). This point, and the implications of the TBW model to the prediction of flow patterns in capillary tubes are demonstrated with reference to Fig. 14.

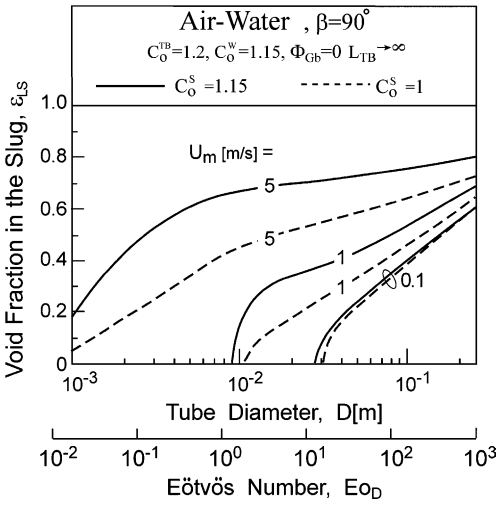

Fig. 13. Effect of tube diameter on the asymptotic ε^w_{LS} and ε^s_{LS} in vertical air–water slug flow.

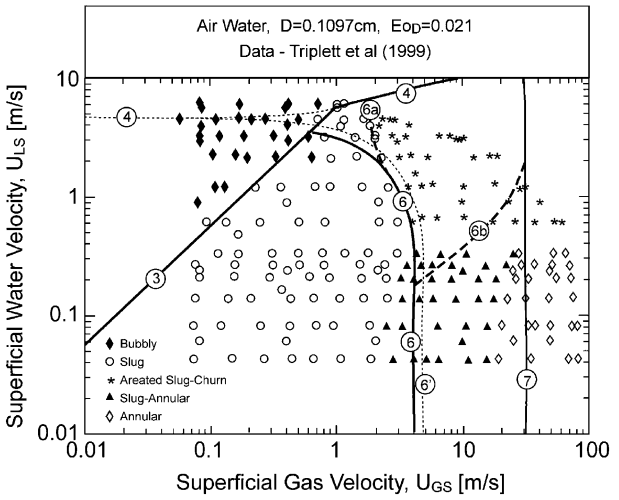

Fig. 14. Flow pattern map for air–water flow in horizontal capillary tube—comparison with the data of Triplett et al. (1999).

Fig. 14 shows the flow pattern map for air–water flow in horizontal 0.1097 cm pipe, $Eo_D = 0.021$. Pictures of flow patterns in this capillary tube verify that the annular configuration is obtained in the TB region (Triplett et al., 1999). The prediction of the bubbly/slug (boundary 3) and slug/dispersed-bubble (boundary 4) transitions are according to Brauner (2001). Boundary 6 corresponds to the minimal mixture velocity for which the Weber number exceeds the We_c. In capillary tubes, the bubbles drift velocities are negligible ($U_0^{TB}, U_0^w \to 0$) and $U_{Lf} \ll U_{LLS} \simeq U_m$. Also the maximal stable bubble diameter is scaled with D ($d_{max} \simeq D/4$) is used. The critical mixture velocity for the onset of bubble entrainment that corresponds to the critical Weber number (Eqs. (7)) is then given by

$$(U_m)_{crit} = 16\left[\frac{\sigma}{\rho_L D}\right]^{1/2} \tag{28}$$

For instance, for $D \simeq 0.1$ cm, the $(U_m)_{crit} \simeq 4$ m/s (boundary 6). It is interesting to note that Eq. (28) yields practically the same value of $(U_m)_{crit}$ as that obtained with the SLB model (Table 1, $Eo_D < 0.2$). The latter is boundary (6′) in the figure. Here again, the similarity results from the fact that in capillary tubes $U_{Lf} \to 0$ and the bubble entrainment is dominated by the velocity of the liquid in the slug. In such cases, models that attribute the TB fragmentation to the turbulence in the slug bulk (as the SLB model) and the TBW model are expected to indicate similar trends.

As shown in Fig. 14, Eq. (28) generally predicts the observed transition from un-aerated slug flow to aerated slug (churn) flow. However, left to boundary (6a), aerated slugs are obtained only with long TB associated with $L_{LS} > 22D$. Such long slugs and TB's may not have been obtained in the 35 cm pipe ($\sim 350D$) used in the experiments. As seen in the figure, this additional consideration improves the prediction of the locus of transition to aerated slugs. Below boundary (6b) the minimal length of the TB (corresponding to short slugs of $L_{LS} < D$) exceeds the length of the pipe. Indeed, this region was identified in the experiment as slug-annular pattern. However, boundary

(6b) implies that in longer tubes slug flow may be obtained in this region. For high U_{GS} the criterion of the onset of drop entrainment from the liquid film (boundary 7) dictates transition to annular flow.

Thus, applying the TBW model can be useful also for the construction of flow pattern maps in capillary systems, where criteria developed for gravity dominated systems (high Eo_D) yield poor predictions (see Triplett et al., 1999). Note, however, that further elaboration of the TBW model is required when it is applied to capillary tubes by accounting for the additional surface tension force in the momentum balances for the undeveloped film zone, as well as the appropriate values for the distribution parameter C_0^{TB}, C_0^{w} and C_0^{s}.

5. Conclusions

The TBW model introduced in this study attributes slug aeration to a recurrent bubble entrainment from the Taylor bubble (TB) tail and their re-coalescence at the successive TB nose. The bubble fragmentation is due to the turbulence in the shear layer and wall jet, which are formed at the TB wake as the liquid film penetrates the slug front. The rate of gas entrainment is determined based on an energy balance between the rate of turbulent kinetic energy and the rate of bubble surface energy production.

The controlling dimensionless parameters that evolve in the model are the Weber number, the Eötvös number, the Froude number in horizontal systems or the film Reynolds number in inclined systems. The latter is related to the TB rise velocity. Also, the Weber number is not based on the mixture velocity, but on the relative velocity between the film and the slug. Therefore, the evaluation of the slug void fraction is coupled with a complete modelling of slug flow.

The TBW model suggests a unified approach for the prediction of the slug void fraction in horizontal, inclined and vertical slug flows. The model has been tested against experimental data available from the literature and was found to predict the effects of liquid and gas flow rates and their physical properties, as well as tube diameter and inclination. The main findings that result from the TBW model are

(a) The rate of bubble entrainment and slug void fraction increase with increasing the upward tube inclination.
(b) In horizontal slug flow, the liquid velocity in the slug dominates the bubble entrainment rate. Therefore, the slug becomes un-aerated as the mixture velocity is reduced below a threshold value. However, in upward inclined slug flow, the bubble entrainment rate is dominated by the liquid film velocity. Therefore, even with a non-zero value for the critical Weber number, aerated slugs can be obtained in the limit of $U_m \to 0$.
(c) The effects of tube diameter and liquid viscosity are very modest in horizontal slug flow, but become much more pronounced as the inclination is increased. In inclined flows, the bubble entrainment decreases with increasing the liquid viscosity and/or with reducing the tube diameter, and increases with reducing the surface tension.
(d) The fully developed film holdup and velocity are approached asymptotically for long TB. Shorter TB's are associated with lower film velocities, and therefore, with lower void fractions in the following liquid slug. Given a two-phase system and mixture velocity, the feasible range

of slug void fraction extends from zero to the asymptotic value. However, fully developed conditions are practically achieved already with finite TB lengths. The finite length decreases as the mixture velocity is reduced and the inclination steepens. In the range of high mixture velocities, however, the TB length effect can be more pronounced than the other influential factors, such as the physical properties, tube diameter and even the inclination.

(e) The holdup in the slug is dependent also on the liquid-cut in the feed. For the same mixture velocity, a higher liquid-cut in the feed is associated with shorter TB's and consequently, with lower values for the slug void fraction.

(f) A distribution in slug lengths, as observed in slug flow, is associated with a distribution of the TB length and thus with distribution in the slug void fraction. This explains the scattering in data of slug void fraction. The model, however, suggests that a short TB that follows a long TB will increase in length, whereas in case it is longer than the preceding TB it will become shorter. In this sense, the bubble entrainment phenomena can be regarded as a mechanism that monitors the TB length distribution. Note that even in case of un-aerated liquid at the front of the TB, it may not dissipate completely, since the bubble entrainment from its tail stops once its length becomes shorter than a threshold value (corresponding to the critical Weber number).

(g) The recurrent bubble entrainment from the TB tail and their re-coalescence at the successive TB nose results in an additional apparent drift. Consequently the effective TB translation velocity is higher than that obtained in un-aerated slug flow. Obviously, this effect become more pronounced as the rate of bubble entrainment increases, in which case the Nicklin et al. (1962) equation is found to underpredict the TB translation velocity.

(h) The higher aeration of the slug in the TB near wake region (compared to the aeration of the far wake region) is commonly attributed to back-flow of part of the bubbles into the TB tail. However, the TBW model indicates that the appearance of a high void fraction region at the TB wake can be a result of the different velocity fields and bubble distributions in the TB wake and in the slug core. These are reflected by different values of the distribution parameter used in the drift-flux model for the bubbly flow in the two regions. The distorted, core-peaked velocity profile in the wake may be associated with a higher distribution parameter compared to the value representing the fully developed velocity profile in the slug core, and consequently higher aeration of the wake region. On the other hand, if similar values of the distribution parameters are used to characterize the bubble flow in the two regions, the predicted void fraction in the slug is insensitive to the values used.

The slug length distribution (or its characteristic length) is still required in the TBW model as a closure to the complete model of slug flow. In un-aerated slugs, the minimal stable slug length is attributed to the length required for the TB wake effects on the velocity field to dissipate and to reach the fully developed velocity profile corresponding to the mixture Reynolds number. In aerated slugs, it is possible that the entrained bubbles will re-coalesce to form a new TB. In this case, the bubble re-coalescence phenomena would control the maximal liquid slug length in the system. This idea is supported by the experimental findings of Felizola and Shoham (1995). They reported a minimal slug length ($\sim 16D$) around 60° inclination (compared to $27D$ and $22D$ in horizontal and vertical slug flow, respectively). Indeed, in this range of tube inclinations, the slip between the bubbles and liquid in the slug is known to be maximal. Re-coalescence can be ex-

pected if the entrained gas rate exceeds the maximal value that the turbulence in the slug bulk can maintain as a stable dispersion. This maximal gas fraction is that offered by bubble fragmentation models that considers the turbulence in the slug bulk (e.g. the SLB models shown in Table 1). However, the modelling of re-coalescence and the implications on the characteristic slug length have not been attempted in this study. Also, it was shown that the modelling of the TB translation velocity is sensitive to the values of the distribution parameters that are used in the drift-flux model for the TB rise velocity and the bubbly flow in the slug. Further research effort is required to establish the effect of the slug void fraction and tube inclination on the appropriate values of the distribution parameters in aerated slug flow. It can be expected that with the development of sophisticated local sensors and data analysis techniques, reliable information concerning the appropriate distribution parameters in aerated slug flow will become available. Updated values will then be incorporated in the TBW model.

Appendix A. Correlation for U_0^{TB} vs. Eo_D

Based on the data of Zukoski (1966), the following correlation was derived (see Fig. 15):

$$C_v^{TB} = \frac{U_0^{TB}}{\sqrt{\frac{\Delta\rho}{\rho_L} gD}} = \begin{cases} 0.35; & \Sigma = \frac{1}{2Eo_D} < 0.1 \\ 0.35e^{-\frac{(\Sigma-0.1)}{0.42}}; & \Sigma \geqslant 0.1 \end{cases} \tag{A.1}$$

The variance of this correlation is 3.5×10^{-3}. In terms of Eo_D, (A.1) reads:

$$C_v^{TB} = \begin{cases} 0.35; & Eo_D > 5 \\ 0.35e^{\frac{(Eo_D-5)}{4.2Eo_D}}; & Eo_D \leqslant 5 \end{cases} \tag{A.2}$$

Eqs. (A.1) or (A.2) are valid for $Re_{TB} = \rho_L U_0^{TB} D/\eta_L > 20$. For lower Re_{TB}, Zukoski (1966, Fig. 4) found that C_v^{TB} is reduced and the values in Fig. 15 should be multiplied by a correction factor, $f_R = 0.224\sqrt{Re_{TB}}$. With this correction, (A.2) yields:

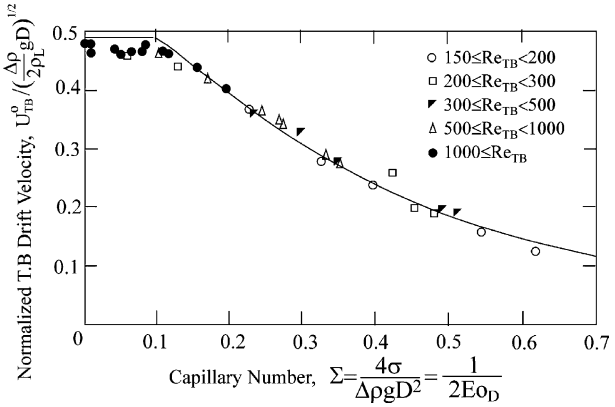

Fig. 15. Comparison of correlation (A.1) for the Taylor bubble rise velocity with the data of Zukoski (1966).

$$\frac{U_0^{\mathrm{TB}}}{(\Delta\rho g D^2/\eta_{\mathrm{L}})} = \begin{cases} 0.0062; & Eo_D > 5 \\ 0.0062\mathrm{e}^{\frac{(Eo_D-5)}{2.1Eo_D}}; & Eo_D \leqslant 5 \end{cases} \tag{A.3}$$

Similar correlations were suggested by Wallis (1969).

Appendix B. Derivation of the differential equation for $\varepsilon_{\mathrm{Lf}}$

Referring to Fig. 1, the continuity equation for the liquid in a coordinate system attached to the rising TB reads:

$$\frac{\partial}{\partial z}\{\rho_{\mathrm{L}}(1-\varepsilon_{\mathrm{GLf}})\varepsilon_{\mathrm{Lf}}(U_{\mathrm{T}\varepsilon}-U_{\mathrm{Lf}})\} = 0 \tag{B.1}$$

The mass conservation of the gas considers the gas flux in the TB and the bubbles in the liquid film. Assuming no-slip between the bubbles and the liquid in the film:

$$\frac{\partial}{\partial z}\{\rho_{\mathrm{G}}\varepsilon_{\mathrm{GLf}}\varepsilon_{\mathrm{Lf}}(U_{\mathrm{T}\varepsilon}-U_{\mathrm{Lf}})+\rho_{\mathrm{G}}\Phi_{\mathrm{GTB}}\} = 0 \tag{B.2}$$

where

$$\Phi_{\mathrm{GTB}} = (U_{\mathrm{T}\varepsilon}-U_{\mathrm{GTB}})\varepsilon_{\mathrm{TB}} \tag{B.3}$$

The momentum balances for the mixture in the film and for the gas flow in the TB are

$$\begin{aligned} &\frac{\partial}{\partial z}\left[\rho_{\mathrm{f}}(U_{\mathrm{T}\varepsilon}-U_{\mathrm{Lf}})^2\varepsilon_{\mathrm{Lf}}\right]+\rho_{\mathrm{G}}\frac{\partial\Phi_{\mathrm{GTB}}}{\partial z}U_{\mathrm{Lf}} \\ &\quad=\frac{\tau_{\mathrm{f}}S_{\mathrm{f}}}{A}-\frac{\tau_{\mathrm{i}}S_{\mathrm{i}}}{A}+\rho_{\mathrm{f}}\varepsilon_{\mathrm{Lf}}g\sin\beta-\rho_{\mathrm{f}}\varepsilon_{\mathrm{Lf}}g\cos\beta\frac{\partial h}{\partial z}-\varepsilon_{\mathrm{Lf}}\frac{\partial P_{\mathrm{if}}}{\partial z} \end{aligned} \tag{B.4}$$

$$\begin{aligned} &\frac{\partial}{\partial z}[\rho_{\mathrm{G}}(U_{\mathrm{T}\varepsilon}-U_{\mathrm{GTB}})^2\varepsilon_{\mathrm{TB}}]-\rho_{\mathrm{G}}\frac{\partial\Phi_{\mathrm{GTB}}}{\partial z}U_{\mathrm{Lf}} \\ &\quad=\frac{\tau_{\mathrm{G}}S_{\mathrm{G}}}{A}-\frac{\tau_{\mathrm{i}}S_{\mathrm{i}}}{A}+\rho_{\mathrm{G}}\varepsilon_{\mathrm{TB}}g\sin\beta-\rho_{\mathrm{G}}\varepsilon_{\mathrm{TB}}g\cos\beta\frac{\partial h}{\partial z}-\varepsilon_{\mathrm{TB}}\frac{\partial P_{\mathrm{iG}}}{\partial z} \end{aligned} \tag{B.5}$$

where ρ_{f} is the density of the mixture in the film:

$$\rho_{\mathrm{f}} = \rho_{\mathrm{L}}(1-\varepsilon_{\mathrm{GLf}})+\rho_{\mathrm{G}}\varepsilon_{\mathrm{GLf}} \tag{B.6}$$

and $\tau_{\mathrm{f}}, \tau_{\mathrm{G}}$ and τ_{i} are the wall shear stresses and the interfacial shear stress respectively. In case the surface tension force due to the interface curvature is negligible, the pressure is the same across the interface, $P_{\mathrm{if}} \simeq P_{\mathrm{iG}}$. Eliminating the pressure gradient from Eqs. (B.4) and (B.5) and utilizing the mass conservation equations (B.1)–(B.3) and Eq. (18), yield the following differential equation for the film holdup:

$$\frac{\mathrm{d}\varepsilon_{\mathrm{Lf}}}{\mathrm{d}\tilde{z}} = \frac{4}{\pi}\frac{\frac{\pi}{4}D(\rho_{\mathrm{f}}-\rho_{\mathrm{G}})g\sin\beta+\frac{\tau_{\mathrm{f}}\widetilde{S}_{\mathrm{f}}}{\varepsilon_{\mathrm{Lf}}}-\frac{\tau_{\mathrm{i}}\widetilde{S}_{\mathrm{i}}}{\varepsilon_{\mathrm{Lf}}(1-\varepsilon_{\mathrm{Lf}})}-\frac{\tau_{\mathrm{G}}\widetilde{S}_{\mathrm{G}}}{(1-\varepsilon_{\mathrm{Lf}})}}{\frac{\pi}{4\widetilde{S}_{\mathrm{i}}}D(\rho_{\mathrm{f}}-\rho_{\mathrm{G}})g\cos\beta-\left[\frac{\rho_{\mathrm{f}}(U_{\mathrm{T}\varepsilon}-U_{\mathrm{Lf}})(U_{\mathrm{GTB}}-U_{\mathrm{Lf}})}{\varepsilon_{\mathrm{Lf}}}+\frac{\rho_{\mathrm{G}}(U_{\mathrm{T}\varepsilon}-U_{\mathrm{GTB}})(U_{\mathrm{GTB}}-U_{\mathrm{Lf}}-\frac{U_{\mathrm{T}\varepsilon}}{\varepsilon_{\mathrm{Lf}}})}{(1-\varepsilon_{\mathrm{Lf}})}\right]} \tag{B.7}$$

where the tilde represents length scales normalized by D. The closure relations used for the shear stresses are given in Eq. (24). The friction factors f_G and f_f are evaluated by $f = CRe^{-n}$ ($n = 1$, $C = 16$ for laminar flow and $n = 0.2$, $C = 0.046$ for turbulent flow, the gas and film Reynolds numbers are calculated based on the hydraulic diameters). The interfacial friction factor f_i for the stratified configuration is taken as $f_i = f_G$ for $\beta = 0$ and $f_i = 0.014$ for inclined flows (Cohen and Hanratty, 1968). For the annular configuration, $f_i = f_G$, and for fully developed film flow it can be evaluated based on Wallis (1969) correlation: $f_i = 0.005(1 + 300\tilde{\delta})$.

Eq. (B.7) can be simplified in case the pressure drop in the film zone is negligible $\frac{\partial P_{lf}}{\partial Z} \simeq 0$. In this case Eq. (B.5) can be ignored and Eq. (B.7) is replaced by

$$\frac{d\varepsilon_{Lf}}{d\tilde{z}} = \frac{4}{\pi} \frac{\frac{\pi}{4} D(\rho_f - \rho_G) g \sin\beta + \frac{\tau_f \widetilde{S}_f}{\varepsilon_{Lf}}}{\frac{\pi}{4\widetilde{S}_i} D(\rho_f - \rho_G) g \cos\beta - \frac{\rho_f (U_{T\varepsilon} - U_{Lf})(U_{GTB} - U_{Lf})}{\varepsilon_{Lf}} + \frac{\rho_G (U_{T\varepsilon} - U_{GTB}) U_{T\varepsilon}}{\varepsilon_{Lf}}} \tag{B.8}$$

Note that in un-aerated slug flow, $U_{T\varepsilon} = U_{GTB}$ and the last term in the denominator of (B.7) (or (B.8)) vanishes.

Appendix C. Estimation of the distribution parameters based on Nuland et al. (1997) data

Depicting Nuland et al. (1997) data for ε_{LS} vs. U_m (Fig. 16a) implies that ε^s_{LS} generally increases with U_m and with the inclination. However, the data appear to be scattered. The data of the slug front translation velocity vs. U_m are shown in Fig. 16b. Assuming the data correspond to

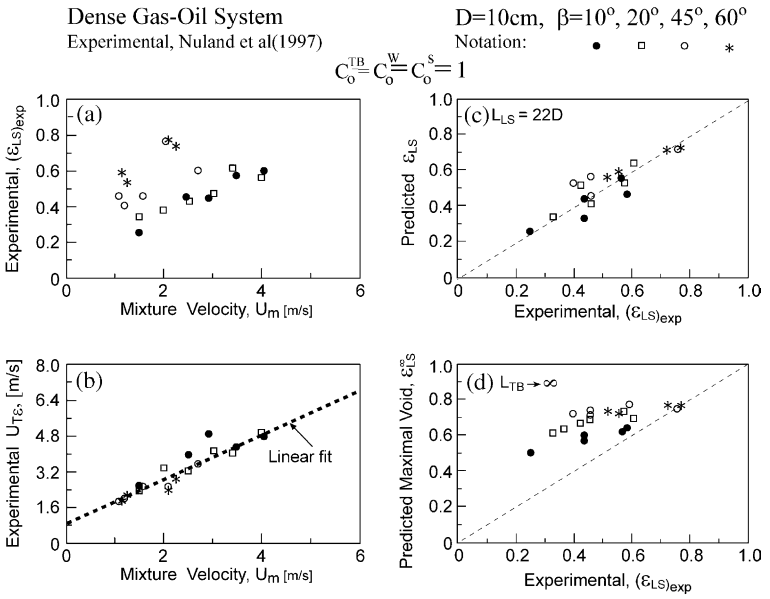

Fig. 16. The TBW model prediction for the slug void fraction obtained with $C_0^{TB} = 1$ for an inclined dense gas–oil system—comparison with experimental data of Nuland et al. (1997).

developed slug flow, the measured values represent $U_{T\varepsilon}$. The best linear fit of $U_{T\varepsilon}$ vs. U_m indicates a slope of about 1. Hence, the TBW model is first applied with $C_0^{TB} = 1$ and assuming a uniform bubble distribution in the TB near and far wake regions ($C_0^w = C_0^s = 1$). The average length of the liquid slug is taken as $22D$.

The predicted values of ε_{LS} (Fig. 16c) favorably compare with the data. Fig. 16d shows the values of ε_{LS} associated with fully developed film flow ($L_{TB} \to \infty$). In this case the predicted values of ε_{LS} overestimate the experimental data. This indicates that, in general, a fully developed film flow cannot be assumed for the TB lengths that satisfy the overall mass balance, Eq. (27), with the typical slug length of $L_{LS} = 22D$. However, comparison of the values obtained for $U_{T\varepsilon}$ and ε_{TB} (not shown) was found to be less favorable. With $C_0^{TB} = C_0^w = C_0^s = 1$ the model generally underpredicts the experimental $U_{T\varepsilon}$ at low inclination (and relatively low U_m) and overpredicts the corresponding ε_{TB}. On the other hand, the data indicate relatively high values of ε_{TB}, accompanied with relatively low $U_{T\varepsilon}$ at steeper inclinations. In view of Fig. 6, these imply $C_0^{TB} > 1$ at shallow inclinations, which decreases at steeper inclinations. This trend of C_0^{TB} is in accordance with recent findings of Van Hout et al., 2002a,b, indicating a minimal value of $C_0^{TB} = 0.95$ at $\beta = 65°$ for air–water slug flow in $D = 2.5$ cm pipe. The appropriate value of the average distribution parameter, $\overline{C}_0 (= C_0^w = C_0^s)$ for characterizing the bubbly flow in the slug, can be evaluated based on Nuland et al. (1997) data on the average void fraction $\bar{\varepsilon}$. The latter is related to the other slug flow parameters by (e.g. Taitel and Barnea, 1990):

$$\bar{\varepsilon} = \frac{U_{GS} - \varepsilon_{LS}(U_{GLS} - U_{T\varepsilon})}{U_{T\varepsilon}} \tag{C.1}$$

Using Eqs. (8) in Eq. (C.1) yields:

$$\overline{C}_0 = \frac{1}{U_m}\left[\frac{U_{GLS} - U_{T\varepsilon}(\bar{\varepsilon} - \varepsilon_{LS})U_{T\varepsilon}}{\varepsilon_{LS}} - U_0(\varepsilon_{LS}, \beta)\right] \tag{C.2}$$

Since $\bar{\varepsilon}, \varepsilon_{LS}$ and $U_{T\varepsilon}$ where measured, Eq. (C.2) can be used with the data to evaluate $\overline{C}_0$. The data imply $\overline{C}_0$ to be insensitive to the inclination, with an average value of $\overline{C}_0 = 1.15(\pm 0.05)$. Accordingly, the results shown in Fig. 7 were obtained when the TBW model is applied with $C_0^{TB} = 1.1, 1.05, 1, 0.95$ at $\beta = 10°$, $20°$, $45°$, $60°$ respectively, and $C_0^w = C_0^s = 1.15$ at all inclinations. No further attempts have been made to optimize the values used for C_0^{TB} (and C_0^w, C_0^s), for obtaining the best comparison with the data of Nuland et al. (1997) as only few data points are available for each inclination.

References

Andreussi, P., Bendiksen, K., 1989. An investigation of void fraction in liquid slugs for horizontal and inclined gas–liquid pipe flow. Int. J. Multiphase Flow 15, 937–946.

Barnea, D., 1987. A unified model for predicting flow-pattern transitions for the whole range of pipe inclinations. Int. J. Multiphase Flow 11, 1–12.

Barnea, D., Brauner, N., 1985. Holdup of liquid slug in two-phase intermittent flow. Int. J. Multiphase Flow 11, 1–12.

Barnea, D., Shemer, L., 1989. Void fraction measurements in vertical slug flow application to slug characteristics and transition. Int. J. Multiphase Flow 15, 495–504.

Bendiksen, K.H., 1984. An experimental investigation of the motion of the long bubbles in inclined tubes. Int. J. Multiphase Flow 10, 467–483.

Bendiksen, K.H., 1985. On the motion of long bubbles in vertical tubes. Int. J. Multiphase Flow 11, 797–812.

Brauner, N., 2001. The prediction of dispersed flow boundaries in liquid–liquid and gas–liquid systems. Int. J. Multiphase Flow 27, 885–910.

Brauner, N., Ullmann, A., 2002. Prediction of holdup in liquid slugs. In: Heat 2002, Third Int. Conf. on Transport Phenomena in Multiphase Flow, IFFM No. 112, pp. 1–15.

Brauner, N., Ullmann, A., 2004. Modelling of gas entrainment from Taylor bubbles. Part B: A stationary bubble. Int. J. Multiphase Flow 30, doi:10.1016/j.ijmultiphaseflow.2003.11.008.

Brauner, N., Rovinsky, J., Moalem Maron, D., 1996. Determination of the interface curvature in stratified two-phase systems by energy considerations. Int. J. Multiphase Flow 22, 1167–1185.

Brauner, N., Moalem Maron, D., Rovinsky, J., 1998. A two-fluid model for stratified flows with curved interfaces. Int. J. Multiphase Flow 24, 975–1004.

Brodkey, R.S., 1969. The Phenomena of Fluid Motions. Addison-Wesley, Reading, MA.

Cheng, H., Hill, J.H., Azzopardi, B.J., 1998. A study of the bubble-to-slug transition in vertical gas–liquid in columns of different diameter. Int. J. Multiphase Flow 24, 431–452.

Cohen, S.L., Hanratty, T.J., 1968. Effects of waves at a gas–liquid interface on a turbulent air flow. J. Fluid Mech. 31, 467–469.

Collins, R., de Moraecs, F.F., Davidson, J.F., Harrison, D., 1978. The motion of large bubbles rising through liquid flowing in a tube. J. Fluid Mech. 89, 497–514.

Delfos, R., Wisse, C.J., Oliemans, R.V.A., 2001. Measurement of air entrainment from a stationary bubble in a vertical tube. Int. J. Multiphase Flow 27, 1769–1787.

Dukler, A.E., Hubbard, M.G., 1975. A model for gas–liquid slug flow in horizontal and near horizontal tubes. Ind. Eng. Chem. Fundam. 14, 337–347.

Dukler, A.E., Moalem Maron, D., Brauner, N., 1985. A physical model for predicting the minimum stable slug length. Chem. Eng. Sci. 4, 1387–1397.

Fabre, J., Liné, A., 1992. Modeling of two-phase slug flow. Ann. Rev. Fluid Mech. 24, 21–46.

Felizola, H., Shoham, O., 1995. A unified model for slug flow in upward inclined pipes. ASME J. Energy Resour. Technol. 117, 1–6.

Fernandes, R.C., 1981. Experimental and theoretical studies of isothermal upward gas–liquid flows in vertical tubes. Ph.D. Dissertation, University of Houston, TX.

Fernandes, R.C., Semiat, R., Dukler, A.E., 1983. Hydrodynamic model for gas–liquid slug flow in vertical tubes. AIChE J. 29, 981–989.

Ferschneider, G., 1983. Ecoulement diphasiques gas–liquide á poches et á bouchons en conduites. Revue de Institute Francais du Pétrole 38, 153–182.

Gomez, L.E., Shoham, O., Taitel, Y., 2000. Prediction of slug liquid holdup: horizontal to upward vertical flow. Int. J. Multiphase Flow 26, 517–521.

Gregory, G.A., Nicholson, M.K., Aziz, K., 1978. Correlation of liquid volume fraction in the slug for horizontal gas–liquid slug flow. Int. J. Multiphase Flow 4, 33–39.

Greskovich, E.J., Shrier, A.L., 1971. Pressure drop and holdup in horizontal slug flow. AIChE J. 17, 1214–1219.

Harmathy, T.Z., 1960. Velocity of large drops and bubbles in media of infinite or restricted extent. AIChE J. 6, 281–288.

Hernandez-Gomez, A., Fabre, J., 2001. An experimental study of the hydrodynamics of a stationary air–water slug. In: Michaelides, E.E. (Ed.), Proc. of the ICMF 2001, 4th Int. Conf. on Multiphase Flow, May 2001, New Orleans, LA, USA.

Heywood, N.I., Richardson, J.F., 1979. Slug flow in air–water mixtures in a horizontal pipe: determination of liquid holdup by gamma-ray absorption. Chem. Eng. Sci. 34, 17–30.

Hibiki, T., Ishii, M., 1999. Experimental study on interfacial area transport in bubbly two-phase flows. Int. J. Heat Mass Transfer 42, 3019–3035.

Hibiki, T., Ishii, M., 2002. Distribution parameter and drift velocity of drift flux model in bubble flow. Int. J. Heat Mass Transfer 45, 707–721.

Hinze, J., 1955. Fundamentals of the hydrodynamic mechanisms of splitting in dispersion processes. AIChE J. 1, 289–295.

Jayanti, S., Brauner, N., 1995. Churn flow—case study. Multiphase Sci. Technol. 8, 471–522.

Kolmogorov, A.N., 1949. On the breaking of drops in turbulent flow. Doklady Akad. Nauk. 66, 825–828.

Malnes, D., 1982. Slug flow in vertical horizontal and inclined pipes. IFE/KR/E-83/002 V. Institute for Energy Technology, Keller, Norway.

Mao, Z.-S., Dukler, A.E., 1989. An experimental study of gas–liquid flow. Expt. Fluids 8, 169–182.

Nicholson, M.K., Aziz, K., Gregory, G.A., 1978. Intermittent two phase flow in horizontal pipes: predictive models. Can. J. Chem. Eng. 56, 653–663.

Nicklin, D.J., Wilkes, J.O., Davidson, J.F., 1962. Two phase flow in vertical tubes. Trans. Inst. Chem. Eng. 40, 61–68.

Nuland, S., Malvik, I.M., Valle, A., Hende, P., 1997. Gas fractions in slugs in dense-gas two-phase flow from horizontal to 60 degrees of inclination. The 1997 ASME Fluids Engineering Division Summer.

Nydal, O.J., Andreussi, P., 1991. Gas entrainment in a long liquid slug advancing in a near horizontal pipe. Int. J. Multiphase Flow 17, 179–190.

Rajaratnam, N., 1976. In: Turbulent Jets, Developments in Water Science, vol. 5. Elsevier, Amsterdam.

Sevik, M., Park, S.H., 1973. The splitting of drops and bubbles in turbulent fluid flow. J. Fluid Eng., Trans. ASME 95, 54–59.

Shacham, M., Cutlip, M.B., 1996. POLYMATH User's Manual, CACHE Corporation, Austin, TX.

Taitel, Y., Barnea, D., 1990. Two phase slug flow. Adv. Heat Transfer 20, 83–132.

Triplett, K.A., Ghiaasiaan, S.M., Abdel-Khalik, S.I., Sadowski, D.L., 1999. Gas–liquid two-phase flow in microchannels. Part I: Two-phase flow patterns. Int. J. Multiphase Flow 25, 377–394.

Van Hout, R., Shemer, L., Barnea, D., 1992. Spatial distribution of void fraction within a liquid slug and some other related slug parameters. Int. J. Multiphase Flow 186, 831–845.

Van Hout, R., Barnea, D., Shemer, L., 2002a. Translational velocities of elongated bubbles in continuous slug flow. Int. J. Multiphase Flow 28, 1333–1350.

Van Hout, R., Gulitski, A., Barnea, D., Shemer, L., 2002b. Experimental investigation of the velocity field induced by a Taylor bubble rising in stagnant water. Int. J. Multiphase Flow 28, 579–590.

Wallis, G.B., 1969. One-Dimensional Two-Phase Flow. McGraw-Hill, New York.

Weber, M.E., 1989. Drift in intermittent two-phase flow in horizontal pipes. Can. J. Chem. Eng. 59, 398–399.

Zaichik, L.I., Alipchenkov, V.M., Avetissian, A.R., 2002. Coalescence and breakup of droplets and bubbles in two-phase turbulent flows. In: Proc. of Heat 2002, The 3rd Int. Conf. on Transport Phenomena in Multiphase Systems, 24–27 June, Baranow, Poland, pp. 511–516.

Zheng, G., 1991. Two-phase slug flow in hilly terrain pipelines, Ph.D. Thesis, The Discipline of Petroleum Engineering, The University of Tulsa, USA.

Zuber, N., Findley, J.A., 1965. Average volumetric concentration in two-phase flow systems. J. Heat Transfer 87, 453–468.

Zukoski, E.E., 1966. Influence of viscosity, surface tension and inclination angle on motion of long bubbles in closed tubes. J. Fluid Mech. 25, 821–837.